Deep–Sea Research I 185 (2022) 103791

Contents lists available at ScienceDirect

Deep-Sea Research Part I

journal homepage: www.elsevier.com/locate/dsri

Variability of deep-sea megabenthic assemblages along the western pathway of the Mediterranean outflow water

Patricia Puerta [a,b,*], Ángela Mosquera-Giménez [c], Olga Reñones [a], Carlos Domínguez-Carrió [d,e], José Luis Rueda [f], Javier Urra [f], Marina Carreiro-Silva [d,e], Jordi Blasco-Ferre [d,e], Yaiza Santana [b,e], Cristina Gutiérrez-Zárate [g], Pedro Vélez-Belchí [c], Jesús Rivera [h], Telmo Morato [d,e], Covadonga Orejas [g]

[a] Centro Oceanográfico de Baleares, IEO, CSIC, Muelle de Poniente, S/N, 07015, Palma de Mallorca, Spain
[b] Save The Med Fundation, Camí de Muntanya 7, 07141, Marratxí, Spain
[c] Centro Oceanográfico de Canarias, IEO, CSIC, Calle La Farola del Mar, 22, 38180, Dársena Pesquera, Santa Cruz de Tenerife, Spain
[d] Instituto de Investigaçao em Ciências do Mar - Okeanos, Universidade dos Açores, 9901-138, Horta, Portugal
[e] IMAR Instituto do Mar, Departamento de Oceanografia e Pescas, Universidade dos Açores, 9901-138, Horta, Portugal
[f] Centro Oceanográfico de Málaga, IEO, CSIC, Puerto Pesquero s/n Fuengirola, 29640, Malaga, Spain
[g] Centro Oceanográfico de Gijón, IEO, CSIC, Avda, Príncipe de Asturias 70 bis, 33212, Gijón, Spain
[h] Instituto Español de Oceanografía, CSIC, Corazón de María, 8, 28002, Madrid, Spain

ARTICLE INFO

Keywords:
Deep-sea benthic habitats
Mediterranean outflow water
Biodiversity
Assemblage structure
Water masses
Cold-water corals
Vulnerable marine ecosystems
Biogeography

ABSTRACT

The presence of different water masses in depth may influence the species distribution and community structure in deep-sea benthic ecosystems. In the North Atlantic, the Mediterranean Outflow Water (MOW) represents an important forcing water mass, whose influence on the distribution of cold-water corals in the northern European margins has been particularly investigated. However, the MOW also spreads westwards into the central North Atlantic bathing several seamounts and seafloor elevations, whose deep-sea benthic communities are still poorly known. In this study, we provide a local to large-scale comprehensive description of deep-sea megabenthic assemblages along the western branch of the MOW, from its origin in the western Mediterranean Sea to the Central North Atlantic close to the Azores archipelago. For some of the studied seafloor elevations, such as Ormonde (Gorringe bank, offshore SW Portugal margin) and Formigas seamounts (SE Azores archipelago), this is the first time these assemblages have been characterized and quantified. The results indicate a strong effect of substrate type in the structure and diversity of the assemblages at local scales; but the effect of water masses becomes more relevant when a large bathymetrical gradient is considered. The results also suggest a potential role of the MOW for biodiversity and biogeographic patterns at the North Atlantic basin, suggesting a potential enhancement of the biodiversity of some deep-sea megabenthic assemblages. Understanding water masses as an integrative tool to delineate biodiversity and biogeographic patterns from local to large scale will contribute to identify different megabenthic assemblages, including vulnerable marine ecosystems, as well as potential regions of refugia under future climate change conditions.

1. Introduction

One of the most outstanding questions in marine ecology is to identify the environmental factors that shape observed patterns of species distributions and, particularly, to what degree the oceanographic parameters shape those patterns (Puerta et al., 2020; Radice et al., 2016; Roberts et al., 2021; Somoza et al., 2021). Temperature and salinity are considered the primary characteristics defining water masses (Bashmachnikov et al., 2015; García-Ibáñez et al., 2015), but also some other parameters might present characteristic signatures in some water masses like concentrations of oxygen, nutrients, etc. (Liu and Tanhua, 2019). These properties might vary temporally and spatially (Liu and Tanhua, 2019; Pollard et al., 2004), but due to the particular values defining each water mass, these can be traced away as they spread from their original

* Corresponding author. Centro Oceanográfico de Baleares, IEO, CSIC, Muelle de Poniente, S/N, 07015, Palma de Mallorca, Spain.
E-mail address: patrix.puerta@gmail.com (P. Puerta).

https://doi.org/10.1016/j.dsr.2022.103791
Received 29 November 2021; Received in revised form 2 May 2022; Accepted 5 May 2022
Available online 14 May 2022

regions of formation (Berglund et al., 2017; Mosquera-Giménez et al., 2019). Water masses can also mix with each other (Fuhr et al., 2021; Liu and Tanhua, 2019), commonly in the boundary regions (Cuny et al., 2002; Sánchez-Leal et al., 2017) or they can maintain similar properties over large areas or time-scales (Emery, 2015; Groeskamp et al., 2019; Raddatz et al., 2014). Thus, the water mass envelop (as a particular combination of oceanographic parameters) becomes an important variable to understand the spatial variability at large-scales in the composition of benthic communities; sometimes with more explanatory power than individual oceanographic parameters (Roberts et al., 2021; Victorero et al., 2018). The presence of distinct water masses has been, indeed, reported as a driver of the distribution of deep-water benthic species and populations at present (Arantes et al., 2009; Dullo et al., 2008; Long and Baco, 2014; Radice et al., 2016; Roberts et al., 2021; Somoza et al., 2014, 2021) and past geological times (Hebbeln et al., 2019; Henry et al., 2014; Raddatz and Rüggeberg, 2019), with large implications in the biodiversity and biogeographic patterns, even at local scales of several hundred meters (Carney, 2005; Puerta et al., 2020 for a review). Improving our knowledge on how water masses can shape the diversity of benthic species in the deep sea is of paramount importance for understanding, the drivers of species present and future species distribution, and for exploring the potential large-scale transport and connectivity of species and populations across large-scale deep-sea regions (Etter and Bower, 2015; Fox et al., 2016; Gary et al., 2020; Henry et al., 2014).

Mediterranean waters flow out close to the bottom through the Strait of Gibraltar into the North Atlantic, becoming the Mediterranean Outflow Water (MOW; Millot, 1999; Sánchez-Leal et al., 2017), a characteristic warm and salty water mass distributed at intermediate depths (~700–1100 m) in the North Atlantic (Candela, 2001; Mosquera-Giménez et al., 2019). In this ocean, the MOW seems to represent an important driver of the distribution of deep-sea cold-water corals (CWCs) along the eastern basin (Dullo et al., 2008; Somoza et al., 2014, 2021) allowing the connectivity with some Atlantic populations (Arnaud-Haond et al., 2017; Boavida et al., 2019; Henry et al., 2014) and promoting the dispersal of Mediterranean species into the Atlantic Ocean (Sitjà et al., 2020). The occurrence of CWC communities along the European margins has been related to the northward pathway of the MOW (De Mol et al., 2005; Dullo et al., 2008; Reveillaud et al., 2008; White and Dorschel, 2010), which also seems to play a key role for dispersal of coral larvae and the (re)colonization of the extinct *Lophelia pertusa* (recently renamed as *Desmophyllum pertusum;* Addamo et al., 2016) in the last post-glacial era (De Mol et al., 2005; Henry et al., 2014). However, another branch of the MOW spreads westwards into the central North Atlantic towards the Azores archipelago (Bashmachnikov et al., 2015; Bozec et al., 2011; Iorga and Lozier, 1999). Along this pathway, the MOW bathes seamounts and seafloor elevations that are still poorly known (Morato et al., 2013; OCEANA, 2005), and which may act as essential "stepping stones" for connecting deep-sea fauna (Breusing et al., 2016; Miller and Gunasekera, 2017; Rowden et al., 2010) between the Mediterranean, the Portuguese margin, the Azores and the Mid-Atlantic Ridge (Gary et al., 2020; Moura, 2015).

This study analyzes patterns in structure and diversity of the deep-sea benthic assemblages along the western branch of the MOW in an attempt to disentangle the role of water mass structure and properties at local and regional scales. For this purpose, we characterized the deep-sea megabenthic assemblages at four seafloor elevations located in the western branch of the MOW along a decreasing gradient of influence towards the central North Atlantic. For some of these seafloor elevations, such as Ormonde (Gorringe bank, offshore SW Portugal margin) and Formigas seamounts (SE Azores archipelago), this study represents the first attempt that characterizes and quantifies their deep-sea megabenthic fauna (>200 m depth). We hypothesized that the structure of different water masses in depth might influence the structure and biodiversity patterns in deep-sea megabenthic assemblages at local and regional scales. While, as reported for the northern (e.g., Boavida et al., 2019; Dullo et al., 2008; Henry et al., 2014) and southern (Somoza et al., 2021) branches of the MOW, the western pathway may also influence the biogeographic patterns by promoting connectivity between Mediterranean and central Atlantic deep-sea communities at regional scale.

2. Material and methods

2.1. Study areas and environmental context

Four geomorphological features that represent different types of seafloor elevations, were investigated in this study, covering a gradient of influence of the Mediterranean Outflow Water (MOW) from the western Mediterranean to the central North Atlantic: The Seco de los Olivos bank (SdO) in the Alboran Sea, the Gazul mud volcano (GMV) in the Gulf of Cádiz, the Ormonde seamount (OS) in the Portuguese margin and the Formigas seamount (FS), SE Azores Archipelago (Fig. 1).

The MOW is an intermediate water mass characterized by a maximum of salinity associated with relatively high temperatures (Fig. 1). It is formed when dense and deep Mediterranean water passes through the Strait of Gibraltar and mixes with the North Atlantic Central Water (NACW; Daniault et al., 1994). Thus, the MOW spreads into the North Atlantic northwards beyond Rockall Trough (Bozec et al., 2011), southwards down to the Canary islands (de Pascual-Collar et al., 2019; Somoza et al., 2021) and westwards as far as Bermuda (Iorga and Lozier, 1999) at an average depth of about 1100 m. This poses MOW as one of the potential key water masses shaping the distribution and connectivity of some marine species (e.g. Patarnello et al., 2007). From the SdO, bathed by the precursor waters of the MOW (i.e., Levantine Intermediate Water), the western pathway of this water mass can be followed throughout these seafloor elevations (Fig. 1), which show similar vertical distribution of water masses (Mosquera-Giménez et al., 2019). The MOW occurs between 400 and 1250 m depth at these seafloor elevations with a salinity range between 27.160 and 27.630 kg m^{-3} (Fig. 1). This maximum shows an intensity decrease from GMV to FS (Mosquera-Giménez et al., 2019, Fig. 1). More details of the MOW characteristics and circulation patterns throughout these features can be found in Mosquera-Giménez et al. (2019) and references therein.

2.1.1. Seco de los Olivos bank

The Seco de los Olivos (also known as Chella) Bank is located in the NE sector of the Alboran Sea, western Mediterranean (Llompart, 1988; Lo Iacono et al., 2012, Fig. 1). Its topography encompasses a main structure formed by a 'guyot' with a flat top summit, surrounded by two ridges at the eastern and western sides (de la Torriente et al., 2019; De Mol et al., 2012; Lo Iacono et al., 2012, 2008, Fig. 2). The bank is made by volcanic rocks covered by mud mixed with fine sand sediment at the bottom (Lo Iacono et al., 2012), covering a total area of approximately 100 km^2 (Lo Iacono et al., 2008). The water column is quite uniform in this region (Fig. 1), with warmer and fresher surface waters of Atlantic origin (Modified Atlantic Water, MAW) in the upper 100 m, over the Levantine Intermediate Water (LIW), a cooler and saltier water mass

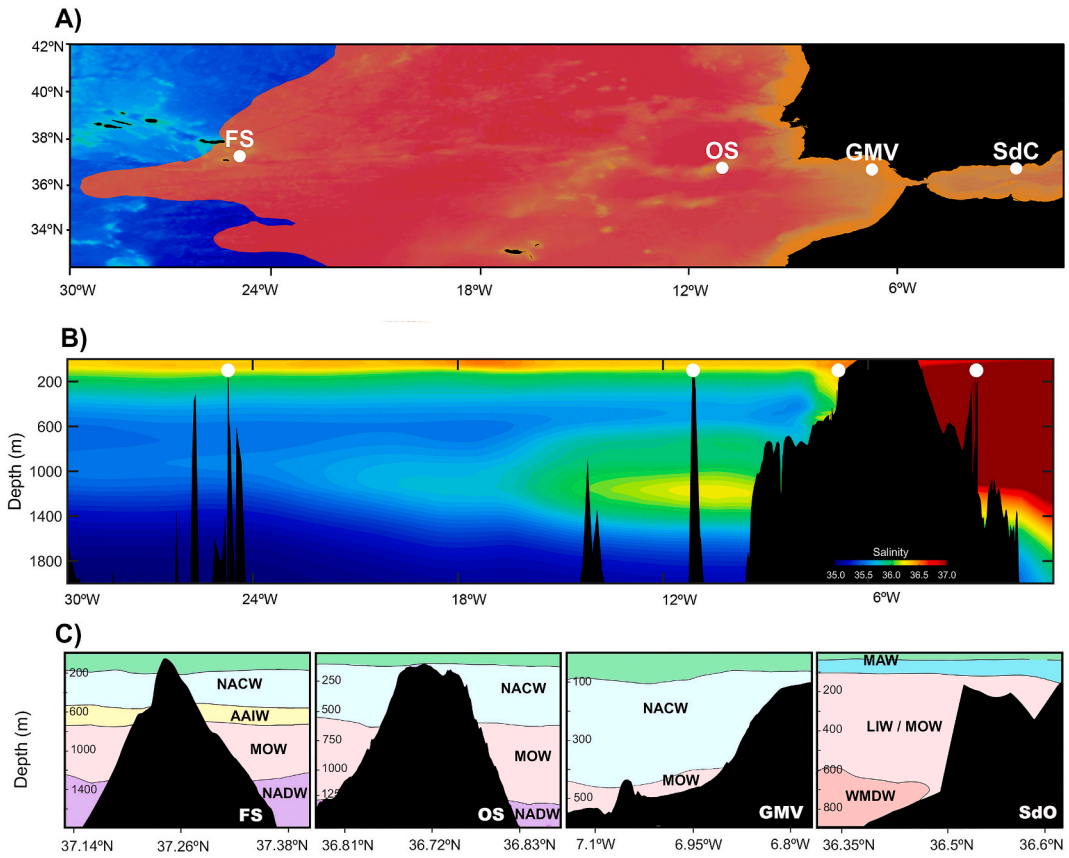

Fig. 1. Location and oceanographic characterization of the seafloor elevations studied along the Mediterranean Outflow Water (MOW) western pathway. The salinity signal of the MOW western pathway can be tracked **A)** geographically and **B)** in the depth profile. **C)** Water masses identified at each of the studied seafloor elevation. Abbreviations: Seco de los Olivos (SdO) bank, Gazul mud volcano (GMV), Ormonde seamount (OS) and Formigas seamount (FS). Modified Atlantic Water (MAW), North Atlantic Central Water (NACW), Antarctic Intermediate Water (AAIW), Mediterranean Outflow Water (MOW), Levantine Intermediate Water (LIW), North Atlantic Deep Water (NADW) and Western Mediterranean Deep Water (WMDW).

with depleted oxygen levels, which represents the main contributor to the characteristics of the MOW. The Western Mediterranean Deep Water (WMDW) flows close to the bottom, below 600 m depth (Gascard and Richez, 1985; Millot, 1999).Table 1.

2.1.2. *Gazul mud volcano*

The Gazul mud volcano is situated in the continental slope of the north-eastern margin of Gulf of Cádiz (Palomino et al., 2016; Urra et al., 2021, Fig. 1), whose shape has been sculpted by tectonics and diapiric processes related to a complex geodynamic evolution of the continental margin (Medialdea et al., 2009). The intense bottom current contributes to the transport and deposition of sediments, seabed erosion and the exhumation of methane-derived authigenic carbonates from the seafloor (Palomino et al., 2016). Indeed, the MOW has carved two depressions at both sides of the mud volcano downstream (Palomino et al., 2016; Rueda et al., 2012; Urra et al., 2021, Fig. 2). The oceanographic circulation is characterized by a two-layer flow (Fig. 1), with the colder and fresher North Atlantic Central Water (NACW) flowing eastwards on the upper layer and, the relative warmer and saltier MOW flowing westwards below 430 m depth to close to the bottom (Mosquera-Giménez et al., 2019; Sánchez-Leal et al., 2017). Nevertheless, a mixed layer of NACW-MOW waters has been observed in the area between approximately 300 and 400 m depth (Sánchez-Leal et al., 2017).

2.1.3. *Ormonde seamount*

Ormonde (Fig. 2) is one of the two seamounts that rises from 5000 m depth at the Gorringe Bank, off SW Cape St. Vincent, Portugal (Ferranti et al., 2014; Xavier and Van Soest, 2007, Fig. 1). It presents a steep SE flank with gullies and incipient canyons. At the SW flank, it is connected through a saddle to the Gettysburg seamount, getting this passage up to 800 m depth (Ferranti et al., 2014). The seamount is mainly composed of deformed mantle rocks, covered by bioclastic material and fine sediments (Ferranti et al., 2014; Xavier and Van Soest, 2007). Below surface waters (Fig. 1), the North Atlantic Central Water (NACW) is characterized by a strong linear relationship between potential temperature and salinity (Mosquera-Giménez et al., 2019). Due to the proximity of the Strait of Gibraltar, there is a sharp increase in salinity and decrease in dissolved oxygen below the NACW at approximately 550m depth, which corresponds to the MOW. Below 1200 m, a lower salinity and higher dissolved oxygen characterize the North Atlantic Deep Water (NADW)

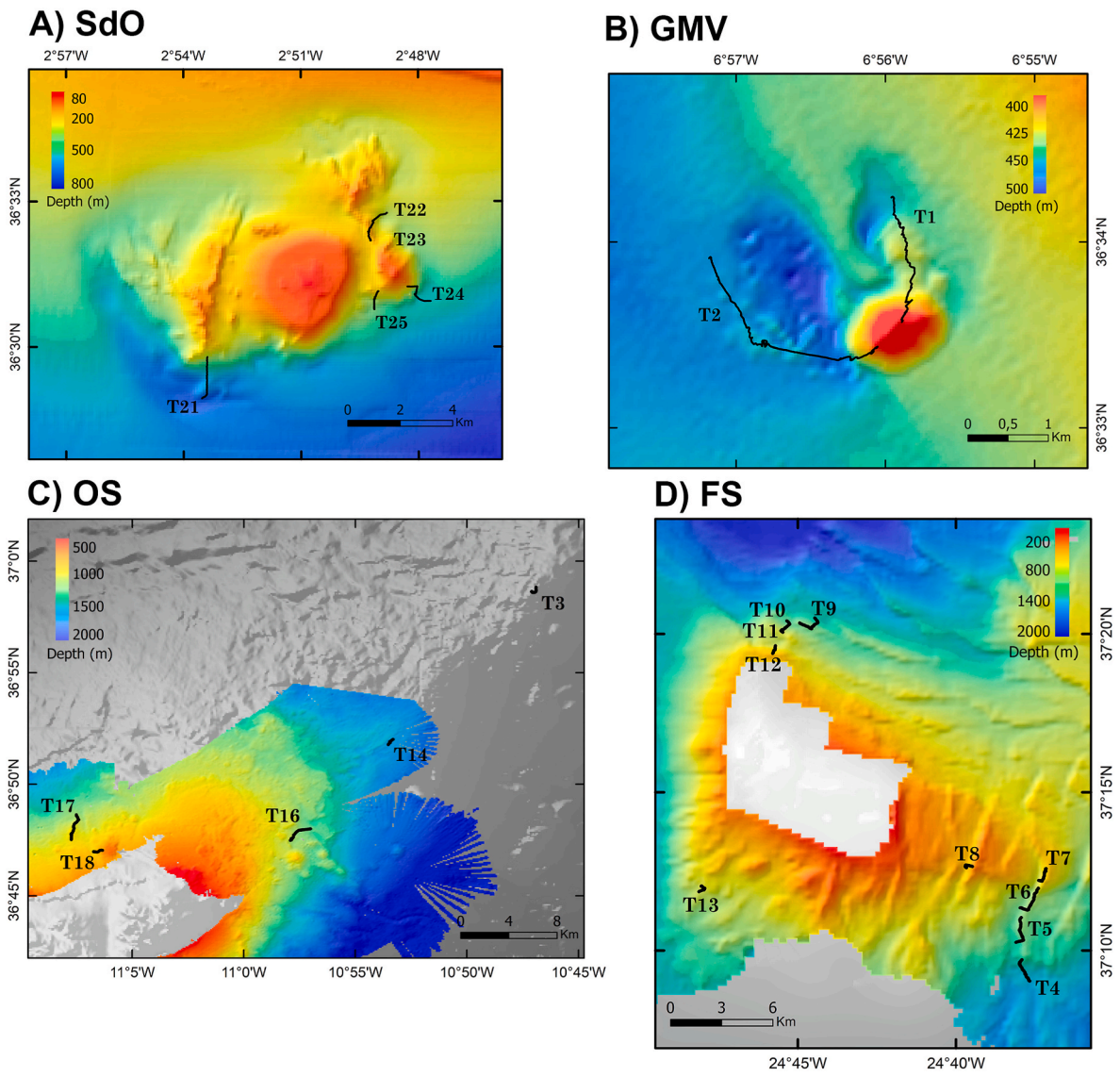

Fig. 2. Bathymetry of the seafloor elevations and location of the ROV video transects. Video transects (T) are numbered in order of performance during the MEDWAVES expedition (Orejas et al., 2017). Abbreviations: Seco de los Olivos (SdO) bank, Gazul mud volcano (GMV), Ormonde seamount (OS) and Formigas seamount (FS).

(Mosquera-Giménez et al., 2019).

2.1.4. *Formigas seamount*

The Formigas seamount is a large submarine volcanic edifice located at the southeastern-most margin of the Azores Plateau (Fig. 1), close to the junction of the East Atlantic Fracture Zone and the Terceira Rift. It is characterized by a horst-and-graben structure, defined by faults, with blocks downthrown towards the east (Ramalho et al., 2018). While evidence of high tectonic activity predominates in the northern sector with different fracture directions, a flat abyssal plain extends to the west at 1800m depth (Abdel-Monem et al., 1975, Fig. 2). The vertical distribution of water masses is similar to thar found in OS (Mosquera-Giménez et al., 2019, Fig. 1), with NACW below the permanent thermocline. However, a third intermediate water mass is present in this seamount, the Antarctic Intermediate Water (AAIW) between the NACW and the MOW. The AAIW generates a region of maximum amplification from the low boundary of the NACW until the core of the MOW, not showing another significant maximum below the 1000 m (Mosquera-Giménez et al., 2019). Thus, a slight decrease in salinity in depth, at approximately 550 m, indicates the presence of diluted AAIW. Salinity increases again in deeper waters from 730 m, corresponding with the influence of the MOW, which here is diluted due to the large distance (~900 nm) from the Strait of Gibraltar. Finally, the constant increase in salinity and temperature towards the bottom indicates the presence of the North Atlantic Deep Water (NADW) below 1250 m.

2.2. *Sampling*

Underwater video footage was acquired during the research expedition MEDWAVES (MEDiterranean out flow WAter and Vulnerable EcosystemS; Orejas et al., 2017), as part of the H2020 European project "A Trans-Atlantic assessment and Deep-Water Ecosystem-Based Spatial Management Plan for Europe" (ATLAS, https://www.eu-atlas.org/). The multidisciplinary expedition took place on September–October 2016 on board the Spanish R/V Sarmiento de Gamboa, targeting the aforementioned seafloor elevations under the influence of the MOW within the Atlantic basin.

The MEDWAVES expedition recorded more than 115 h of video footage along 25 ROV transects in the four seafloor elevations previously described (Fig. 2). These video transects were performed with the ROV

Table 1
Summary of the ROV video transects conducted during the MEDWAVES expedition. See Fig. 2 for the location of the video transects. Depth range is indicated from the starting to the end value of the corresponding ROV transect. Transect numbers are indicated as in MEDWAVES expedition report (Orejas et al., 2017). (*) ROV video transects aborted due to technical issues.

Orientation	Depth (m)	Start location (lat, lon)	End location (lat, lon)	Distance (m)	Duration (hh:mm)	Transect
Seco de los Olivos bank						
N	250–238	36.539°N, 2.821°W	36.537°N, 2.820°W	461	03:12	23
N	446–285	36.513°N, 2.818°W	36.519°N, 2.817°W	897	03:53	25
N	693–330	36.482°N, 2.892°W	36.496°N, 2.890°W	1764	04:34	21
W	385–250	36.546°N, 2.813°W	36.539°N, 2.821°W	1256	03:33	22
SE	560–230	36.516°N, 2.795°W	36.521°N, 2.805°W	1585	04:02	24
SE	793–705	36.478°N, 2.895°W	36.482°N, 2.893°W	443	01:42	19*
Gazul mud volcano						
E	467–385	36.571°N, 6.933°W	36.559°N, 6.931°W	1806	06:18	1
W	480–400	36.565°N, 6.953°W	36.557°N, 6.934°W	3125	08:39	2
Ormonde seamount						
N	872–680	36.783°N, 11.112°W	36.784°N, 11.106°W	687	02:18	18
NE	1158–921	36.811°N, 11.125°W	36.811°N, 11.125°W	2487	07:10	17
NE	1242–1076	36.800°N, 10.950°W	36.791°N, 10.965°W	2163	05:15	16
NE	1547–1524	36.866°N, 10.888°W	36.866°N, 10.888°W	724	04:55	15*
NE	1960–1909	36.977°N, 10.785°W	36.980°N, 10.782°W	1013	08:44	3
Formigas seamount						
NW	1030–679	37.327°N, 24.762°W	37.323°N, 24.763°W	549	04:11	12
NW	1175–1029	37.336°N, 24.757°W	37.334°N, 24.758°W	559	04:23	11
NW	1332–1173	37.340°N, 24.756°W	37.336°N, 24.756°W	590	02:29	10
NW	1419–1180	37.342°N, 24.741°W	37.339°N, 24.749°W	1703	06:53	9
SE	759–479	37.210°N, 24.661°W	37.211°N, 24.658°W	559	02:22	8
SE	1004–754	37.203°N, 24.623°W	37.210°N, 24.619°W	1117	04:10	7
SE	1260–921	37.189°N, 24.633°W	37.199°N, 24.623°W	1940	07:34	6
SE	1360–1174	37.171°N, 24.635°W	37.184°N, 24.632°W	1866	05:18	5
SE	1580–1343	37.115°N, 24.628°W	37.162°N, 24.632°W	1725	05:57	4
S	1045–957	37.198°N, 24.802°W	37.200°N, 24.801°W	785	03:28	13

(Super Mohawk model) Liropus 2000, which was equipped with Kongsberg (10 Mpx, 3648 x 2736 resolution) still image and (color zoom, monochrome and low light vision) video cameras. An additional HD video camera was mounted to record high quality footage to be used for image analysis of benthic megafauna. The illumination was provided by Sealite Spheres and the corresponding flash lights of each camera. Throughout the transects, a pair of parallel laser beams mounted 10 cm apart was used to scale images and calculate the transect width and sampling area. The positioning of the ROV was recorded using the HYPACK software. The ROV was also equipped with a CTD sensor, which collected temperature, salinity pressure and dissolved oxygen data at every second of the video footage. More technical details of ROV equipment can be found in Orejas et al. (2017). The ROV transects were not evenly distributed among the studied seafloor elevations, since more effort was invested in the less explored areas at the time (Table 1; Fig. 2). Therefore, to gather the most representative data possible, different bathymetrical ranges and geographical orientations were targeted at the different seafloor elevations, aiming to obtain a comprehensive overview of their inhabiting benthic assemblages and the influences of water masses (Table 1). The (two) transects aborted due to technical issues were not included in the analyses (Table 1).

2.3. Image processing

To obtain quantitative biological data comparable across transects and studied seafloor elevations, a series of still images were captured from the video footage at 5 m intervals using the software OFOP (Ocean Floor Observation Protocol) v3.6. This software allows coupling the video footage with ROV navigation data and thus, extracting georeferenced still images at each transect. This methodology has been previously used in other studies to identify spatial patterns in megabenthic assemblages (e.g., Bo et al., 2011; Ramos et al., 2016). From the 23 valid video transects performed during the MEDWAVES cruise, a total of 5732 still images were obtained, with an average of 1433 ± 545 images per transect (Supp.1). Images with poor quality (i.e., sediment resuspension, lack of focus, ROV too far from the seafloor, close-ups for species identifications and not visible lasers, sampling events) were disregarded for the analyses. Since the ROV did not move at a fixed distance from the seabed constantly, the area covered by the still images was variable. Thus, to standardize the sampled area across all still images and transects, only images with a width range between 1.5 and 2.5 m were selected for quantitative analyses, ensuring robust comparisons. The final number of still images used for statistical analysis was approximately 44% of the original set of images extracted from the video footage (Supp. 1).

Annotations of substrate type and megabenthic species were made on every selected still image using the software PAPARA(ZZ)I (Marcon and Purser, 2017). Due to the orientation of the cameras when recording the video transects, the top area of the still images (~1/4 of the image) frequently presented poor visibility (Supp. 2) and was excluded from the annotation process to reduce potential misidentification of the organisms (Supp. 2). Substrate type was determined and quantified (in %) by overlapping a grid of 20 cells on the useable area of every still image. Each cell was assigned to a substrate category, allowing to objectively estimate the percentage of different substrate types in mixed bottoms. Substrate categories were kept as simple as possible based on the classifications of previous works (e.g., Howell, 2010; Porteiro et al., 2013; van den Beld et al., 2017), and included: mud, sand, detritic, soft-flagstone, hard-flagstone, sandy gravels, pebbles and rock. Mud was identified as the softest sediment, with very fine grains, undistinguishable in the images; while sand presented discernible grain-size. Detritic was defined as coarse size sand with bioclastic components. Hard-flagstone identified layers of compact sediment with the morphology of a thick platform containing slabs and cracks; while

Table 2
List of the Operational Taxonomic Unit (OTU) identified in the present study and the number of individuals or colonies recorded at each of the seafloor elevations, including only the standardized images from ROV video transects retained for the statistical analyses. Abbreviations: Seco de los Olivos (SdO) bank, Gazul mud volcano (GMV), Ormonde seamount (OS) and Formigas seamount (FS).

Phylum	Group	OTU	SdO	GMV	OS	FS
Brachiopoda						
	Brachiopoda	Brachiopoda	0	0	0	1
Bryozoa						
	Bryozoa	Bryozoa 1	0	0	0	6
		Bryozoa 2	0	0	0	1
		Bryozoa 3	0	0	0	3
Cnidaria						
	Actiniaria	*Actinauge richardi*	0	1117	0	0
		Actiniaria 1	0	0	1	0
		Actiniaria 2	0	0	0	1
		Actiniaria 3	0	0	0	14
		Anthozoa 3	0	0	1	0
		Anthozoa 4	0	0	1	0
	Alcyonacea	*Acanella arbuscula*	0	0	12	233
		*Acanthogorgia armata**	0	0	0	160
		Acanthogorgia spp.	86	245	0	0
		Alcyonacea	0	0	1	0
		Alcyonacea 1	0	0	0	2
		Alcyonacea 5	0	0	0	8
		Alcyonacea 6	17	0	0	0
		Alcyonacea 7	0	0	0	6
		Alcyonacea 8	0	0	22	0
		Anthothelidae	0	0	0	2
		cf. *Anthomastus*/cf. *Pseudoanthomastus* sp.	0	0	0	13
		Bebryce mollis	0	10	0	0
		Callogorgia verticillata	1	2	0	0
		Candidella imbricata	0	0	0	158
		Chelidonisis aurantica	0	0	0	16
		Chrysogorgia sp.	0	0	0	55
		Enallopsammia rostrata	0	0	0	1
		Gorgonacea	0	0	22	0
		Gorgonian 1	0	0	1	0
		Hemicorallium niobe	0	0	0	5
		Hemicorallium tricolor	0	0	0	43
		Iridogorgia cf. *fontinalis*	0	0	0	13
		Isidiidae	0	0	0	1
		Keratoisis sp.	0	0	0	11
		Lateothela grandiflora	0	0	0	3
		Lepidisis sp.	0	0	0	1
		Narella bellissima	0	0	1	444
		Narella versluysi	0	0	13	670
		Paramuricea sp.	0	0	0	1
		Placogorgia sp.	0	0	11	0
		Pleurocorallium johnsoni	0	0	0	2
		Plexauridae 1	0	0	0	2
		Plexauridae 2	0	15	0	14
		Plexauridae 3	0	0	0	402
		Plexauridae 4	0	0	0	3
		Plexauridae 5	0	0	0	8
		Radicipes cf. *gracilis*	0	0	0	16
		Swiftia sp.	0	0	1	34
		Thouarella sp.	0	0	0	6
	Antipatharia	Anthipatharia 3	0	0	0	1
		Antipathes sp.*	0	0	0	17
		Antipathes cf. *erinaceus*	0	0	0	6
		Bathypathes spp*	0	0	0	8
		Bathypathes sp 1	0	0	2	0
		Leiopathes cf. expansa	0	0	0	56
		Leiopathes glaberrima	0	1	0	0
		Parantipathes hirondelle	0	0	0	6
		Parantipathes sp.	17	0	8	0
		Stichopathes sp.	0	0	26	16

(*continued on next page*)

Table 2 (*continued*)

Phylum	Group	OTU	SdO	GMV	OS	FS
	Ceriantharia	Ceriantharia	2	0	2	17
	Hydrozoa	*Crypthelia* sp.	0	0	0	20
		Hydrozoa spp	0	13	3	0
		Hydrozoa 1	0	0	0	3
		Hydrozoa 5	0	0	0	3
		Hydrozoa 6	0	0	0	35
		Stylasteridae spp	0	3	0	0
		Stylasteridae 1	0	0	0	3
		Stylasteridae 2	0	0	0	3
	Pennatulacea	cf. *Gyrophyllum hirondellei*	0	0	0	4
		Kophobelemnon sp.	9	0	0	0
		Pennatulacea 1	1	0	0	0
		Pennatulacea 2	0	0	1	0
	Scleractinia	*Caryophyllia* sp.	0	6	0	31
		Cup coral 1	0	0	2	0
		Cup coral 2	0	0	1	0
		Dendrophyllia cornigera	26	3	0	0
		Desmophyllum dianthus	0	0	0	11
		Flabellum chunii	0	62	0	0
		Flabellum sp.	0	0	0	1
		Leptopsammia formosa	0	0	0	129
		Lophelia pertusa	0	7	0	48
		Madrepora oculata	4	94	0	18
		Scleractinia 1	0	0	1	0
		Solenosmilia variabilis	0	0	1	0
	Zoantharia	Zoanthidae	0	0	0	1
Chordata						
	Teleosteii	*Anthias anthias*	1	0	0	0
		Bathypterois phenax	0	0	0	1
		Callionymus sp.	1	0	0	0
		Capros aper	1	0	0	0
		Chaunax sp.	0	0	0	1
		Coelorinchus caelorhincus	4	0	0	0
		Gadiculus argenteus	91	1	0	0
		Gadomus longifilis	0	0	0	1
		Helicolenus dactylopterus	20	1	0	0
		Hoplostethus atlanticus	0	0	0	2
		Hoplostethus mediterraneus	2	0	13	0
		Hymenocephalus italicus	1	0	0	0
		Lophius piscatorius	0	0	0	1
		Macrouridae 5	0	0	0	1
		Macrouridae 6	0	0	0	2
		Macrouridae 7	0	0	0	1
		Micromesistius poutassou	1	0	0	0
		Mora moro	0	0	3	0
		Neocyttus helgae	0	0	0	5
		Nettastomatidae 1	0	0	0	1
		Pagellus bogaraveo	1	0	0	0
		Phycis blennoides	1	0	0	0
		Phycis sp.	0	0	0	1
		Polyacanthonotus rissoanus	0	0	0	1
		Polyacanthonotus sp.	0	0	1	0
		Scorpaena elongata	5	0	0	0
		Synaphobranchus sp.	0	0	9	8
		Trachurus trachurus	19	0	0	0
		Trachyscorpia cristulata	0	0	0	1
	Morphotype	eel fish 1	0	0	1	0
		eel fish 2	0	0	4	0
		eel fish 4	0	0	0	1
		fish 1	0	0	0	1
		fish 2	0	0	0	3
		fish 3	3	0	0	0
	Tunicata	*Polycarpa* sp	0	67	0	0

(*continued on next page*)

Table 2 (*continued*)

Phylum	Group	OTU	SdO	GMV	OS	FS
Arthropoda: Crustacea						
	Cirripedia	Cirripedia	0	0	0	125
	Decapoda	*Palinurus mauritanicus*	0	1	0	0
		Galatheoidea	4	16	1	4
		Pagurus spp.	1	0	1	0
		Chaceon affinis	0	0	0	2
		Paramola cuvieri	0	0	0	1
		Plesionika spp.	4	0	0	0
		Aristaeopsis edwardsiana	0	0	2	0
		Shrimp 1	0	0	20	1
		Shrimp 2	0	0	3	0
		Shrimp 4	0	0	0	3
Echinodermata						
	Asteroidea	Asteroidea 1	0	0	0	2
		cf. *Evoplosoma* sp.	0	0	0	1
		Pteraster personatus	0	0	0	6
		Asteroidea 4	0	0	1	0
		Asteroidea 5	0	0	3	0
		Brisingella coronata	6	0	0	0
		Chaetaster longipes	0	2	0	0
	Crinoidea	Crinoidea	0	81	3	21
		Stalk crinoidea	0	0	3	4
	Echinoidea	*Cidaris* sp.	5	51	0	17
		Echinoidea	0	1	0	1
		Echinus melo	1	0	0	0
		Gracilechinus acutus	0	5	0	0
	Holothuroidea	*Mesothuria intestinalis*	3	0	0	0
		Parastichopus regalis	1	1	0	0
	Ophiuroidea	*Gorgonocephalus caputmedusae*	0	0	0	2
		Ophiuroidea	0	2	13	13
Foraminifera						
	Foraminifera	cf. *Syringammina fragilissima*	0	0	0	28
Mollusca						
	Bivalvia	Bivalvia	0	2	0	7
	Cephalopoda	*Eledone cirrhosa*	0	5	0	0
	Gastropoda	*Charonia lampas*	1	0	0	0
		Gastropoda	0	1	1	0
		Nudibranchia	0	0	2	0
Porifera						
	Demospongia	*Cladocroce* sp.	33	0	2	0
		Geodia spp.	0	0	1	0
		Haliclona magna	0	0	0	1
		Hymedesmia sp.	0	0	0	5
		Leiodermatium sp.	0	4	1	0
		Macandrewia azorica	0	0	0	3
		Poecillastra compressa (white variety)*	0	0	0	4
		Pachastrella sp.	6	37	8	0
		Phakellia sp.	14	0	1	0
		cf. *Phakellia ventilabrum*	0	0	0	2
		Desmacella grimaldii	0	0	0	157

(*continued on next page*)

Table 2 (*continued*)

Phylum	Group	OTU	SdO	GMV	OS	FS
		Rhizaxinella sp.	10	0	0	0
		Stylocordyla pellita	20	0	6	192
		Thenea sp.	0	0	128	0
	Hexactinellida	*Aphrocallistes beatrix**	0	0	0	1
		Aphrocallistes sp.	0	0	4	0
		Asconema setubalense	14	12	2	0
		Asconema sp.	0	0	1	3
		Farrea occa	0	0	0	154
		Hyalonema sp.	0	0	15	0
		Pheronema carpenteri	0	0	5	39
		Regadrella phoenix	0	0	0	1
		Rossellidae	0	0	5	2
	Morphotype	Porifera	1	0	3	0
		Porifera arborescent [a]	0	0	0	1
		Porifera digitate	1	0	436	0
		Porifera digitate 1[a]	0	0	0	1821
		Porifera digitate 2	0	0	0	61
		Porifera digitate 3	0	0	0	64
		Porifera encrusting 1	0	0	0	82
		Porifera encrusting 2	7	0	0	0
		Porifera encrusting 3	0	0	0	34
		Porifera encrusting 4	0	0	13	0
		Porifera encrusting 5	0	0	0	4
		Porifera encrusting 6	0	0	202	44
		Porifera encrusting 7	0	0	0	37
		Porifera encrusting 8	0	5	2	0
		Porifera encrusting 9	0	0	0	59
		Porifera encrusting 10	0	0	0	729
		Porifera encrusting 11	214	0	353	432
		Porifera fistulose	0	0	32	46
		Porifera flabellate	0	0	0	1
		Porifera glass	3	0	4	0
		Porifera glass 1	0	0	2	0
		Porifera glass 2	0	0	0	33
		Porifera glass 3	0	0	6	3
		Porifera glass 4	0	0	1	0
		Porifera glass 5	0	0	66	0
		Porifera globular	0	12	3	51
		Porifera lamellate	14	1	9	0
		Porifera lamellate 1	0	0	10	0
		Porifera llamelate 2	0	0	0	2
		Porifera massive	17	172	270	11
		Porifera massive 1	0	9	0	0
		Porifera massive 2	0	4	0	0
		Porifera massive 3	0	11	0	0
		Porifera massive 4	0	95	0	0
		Porifera pedunculate	0	2	0	0
		Porifera pedunculate 1	0	0	0	48
		Porifera pedunculate 2	0	0	0	7
		Porifera pedunculate 3	1	0	0	0

[a] OTU under study since it may encompass more than one different OUT or species level identification present some uncertainty. Further research is still in progress.

soft-flagstone denoted incipient slabs, whose sediment is not completely compacted yet. A mixed substrate observed in OS formed by sand and large gravels was defined as an independent substrate category due to the impossibility of defining accurate percentages of each of these two mixed substrate types. Occurrence of megabenthic fauna larger than 5 cm was annotated and identified to the lowest possible taxonomic level. When the identification at species level was not possible or reliable, taxa were classified in higher taxonomic levels (e.g. genus, family, phylum) and/or classified as morphotypes (e.g., Porifera tubular, Porifera encrusting purple, Gorgonia white). Therefore, the taxonomic inventory used (Table 2) relies on Operational Taxonomic Units (OTUs; e.g., Howell et al., 2019; Lacharité and Metaxas, 2017) rather than species, which comprises identifiable entities at different taxonomic levels. The list of OTUs was homogenized across the four studied seafloor elevations (Table 2).

2.4. Data analyses

2.4.1. Assemblage structure

Differences in composition and structure of the megabenthic assemblages were analysed at each seafloor elevation using multivariate dimension reduction techniques. We primarily applied non-Metric Multidimentional Scaling (nMDS) analysis for this purpose. This ordination and reduction dimension technique can handle non-linear responses, being very robust with respect to zero-zero species density pairs and effective finding underlying gradients (Paliy and Shankar, 2016). The nMDS was performed on a Bray-Curtis dissimilarity matrix, setting dimensions to the minimum possible in each case. The nMDS biplot represents the pairwise dissimilarities in OTU composition among sampled sites, i.e., each still image, with ordination axes do not corresponding to any particular gradient in the original dataset. To explain the results of nMDS ordinations, environmental variables (including percentage of substrate, temperature, salinity, dissolved oxygen and

water density) were fitted onto the ordination axes using a generalized additive model (GAM). The environmental fitting was tested for significance by means of 1000 permutations. Different number of dimensions, random starting points and a maximum of 400 configurations were tested in the nMDS analyses. Only the OTUs with at least 5 records at a given seafloor elevation were included in these analyses. When sample size is small, nMDS analysis might present issues related to the stress value, which is associated with the goodness of fit of the outputs. In such cases, metric or ordinary MDS (also known as principal coordinates analysis, PCoA) was applied instead (Paliy and Shankar, 2016). Each PCoA is a linear combination of original variables (i.e., OTUs) that produces the largest dispersion of values along this component and they are calculated as orthogonal to the preceding components (Paliy and Shankar, 2016). Multivariate ordination methods were performed in R software, version 3.4.4 (R Core Team, 2020) using the package *vegan* (Oksanen et al., 2019).

2.4.2. Diversity measurements

Diversity measurements based on the identified OTUs, were calculated for each seafloor elevation by water mass and main substrate type (hereafter refer as assemblage categories), using Hills numbers (Chao et al., 2014a) and their corresponding rarefaction/extrapolation (R/E) curves (Chao et al., 2014b). This method accounts for bias related to the true number of species and unbalanced sampling (Chao et al., 2014a). To balance the number of assemblage categories to be compared (i.e., water masses-substrate type combinations) and the sample size at each category, maintaining the differences between soft and hard bottom assemblages; we grouped the eight substrate types described above into consolidated and semi-consolidated or hereafter refer as “hard” (i.e., rock, hard-flagstone and detritic) and sedimentary ones, hereafter refer as “soft” (i.e, mud, sand, soft-flagstone, sandy gravels and pebbles) substrate categories, based on the observations of the present study and expert opinions. Similar classifications have been used in previous studies (e.g., van den Beld et al., 2017; Wienberg et al., 2013). Thus, diversity measurements were calculated for these two substrate categories in each water mass depth interval (e.g., MOW, NACW, etc.) at every seafloor elevation. The different measurements of diversity defined by Hill numbers are parameterized by the same function (see more details in Chao et al., 2014a), only differing in the exponential order q, which determines the sensitivity of the diversity measurement to species relative abundances. These measurements are the counterparts of three of the most widely used biodiversity indices such as, species richness ($q = 0$), Shannon ($q = 1$) and inverse Simpson indices ($q = 2$). These indices calculated as Hill numbers are expressed as effective number of species (or OTUs at the present study), and therefore diversity is directly comparable across indices and/or groups, regions, etc. (Chao et al., 2014a). The R/E curves were extrapolated to double the size of the smallest reference sample at maximum. Partitioning diversity was also explored using Hill numbers (Chao et al., 2014a; Jost, 2007); which accurately reflect the compositional similarity of different assemblages based on the diversity relationship *gamma* = *alpha* x *beta*. Thus *gamma-diversity* define total diversity of all assemblages pooled together; which can be decomposed into the independent components *alpha-*(diversity as number of species within an assemblage) and *beta-diversity* (effective number of distinct assemblages; Jost, 2007). Hill numbers and the R/E curves were calculated using the R package ‘iNEXT’ (Hsieh et al., 2016); while partitioning diversity used the package ‘hillR’ (Li, 2018).

3. Results

3.1. Composition of the megabenthic assemblages

A total of 11,883 individuals/colonies belonging to 216 OTUs (Table 2) were recorded from the final set of 2488 standardized still images (SdO = 489, GMV = 355, OS = 615, FS = 1029). Overall, the four studied seafloor elevations showed differences in the composition of the assemblages in terms of the occurrence of the main taxonomic groups. Most benthic assemblages were clearly dominated by structuring OTUs such as sponges (Porifera) and corals *sensu lato* (Cnidaria) in both,

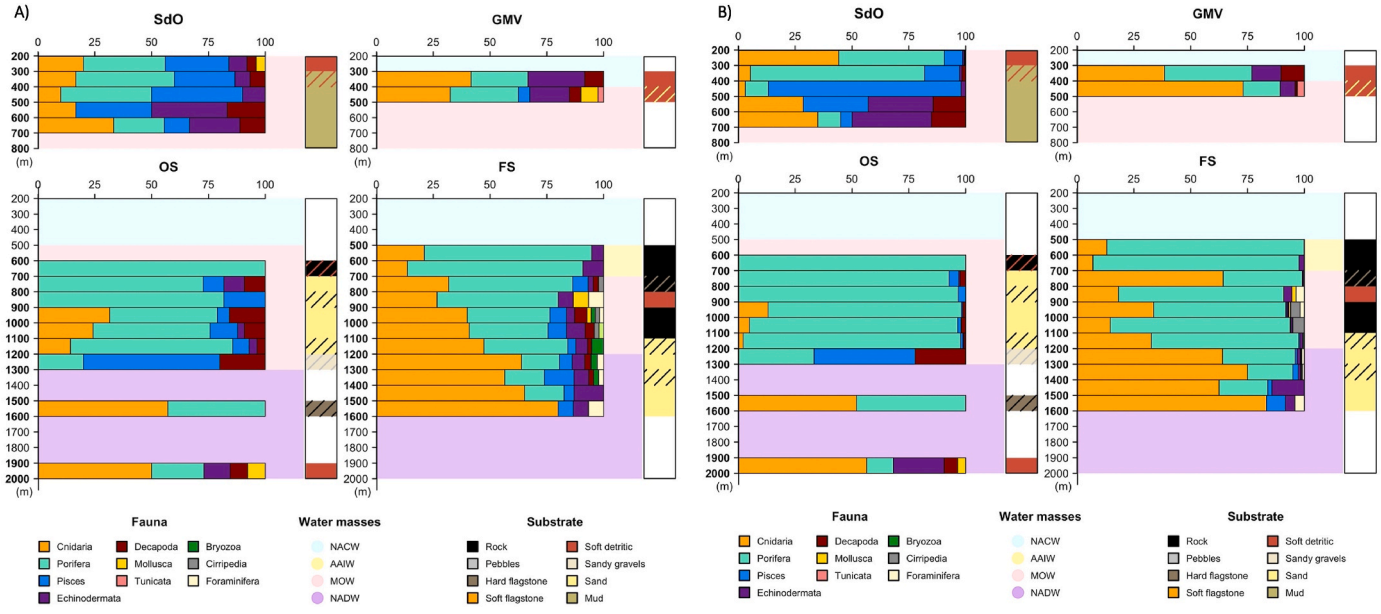

Fig. 3. Composition and structure of the deep-sea megabenthic assemblages observed at the four studied seafloor elevations: Seco de los Olivos (SdO) bank, Gazul mud volcano (GMV), Ormonde seamount (OS) and Formigas seamount (FS). **A)** Relative richness of Operational Taxonomic Units (OTUs) and **B)** relative abundance by taxonomic group. The x-axis shows percentages of the fauna composition. The y-axis shows depth in meters, the bathymetrical range explored by the ROV transects is denoted in bold. Note that in OS the explored depths ranges were not continuous. Distribution of the water masses at depth is shown by the background colors of the plot area, including North Atlantic Central Water (NACW), Antarctic Intermediate Water (AAIW), Mediterranean Outflow Water (MOW) and North Atlantic Deep Water (NADW). Vertical bars on the right side of each plot show dominant substrate at the corresponding depth; when substrate type was mixed, the secondary substrate (>25% and <50% coverage) was denoted by strip lines on top of the primary substrate.

number of OTUs and total abundance (Fig. 3). The diversity of cnidarians was generally high in terms of number of OTUs across all seafloor elevations (from 9 in SdO up to 54 OTUs in FS), being gorgonians (Alcyonacea) the most frequent and abundant group of cnidarians, particularly in FS, followed by stony (Scleractinia) and black (Antipatharia) corals. Other groups of cnidarians, such as sea-pens and actinarians, were scarce with the exception of the hormathiid actinarian *Actinauge richardi* (Table 2) in GMV. Most of the OTUs within the Phylum Porifera were identified as morphotypes, also displaying high diversity in terms of number of OTUs (Fig. 3; from 12 in GMV up to 34 OTUs in FS). Encrusting and massive Porifera morphotypes were the most abundant in all the studied seafloor elevations, with a notable presence of the morphotypes "Porifera glass" in OS and "Porifera digitate" in FS.

The variability of the observed assemblages was partly associated with the presence of different substrate types, being dominant taxonomic groups different at each seafloor elevation (Fig. 3). Large extensions of muddy habitats were mainly found in SdO, where Porifera presented higher abundance, followed by demersal fish and Cnidaria at similar proportions (~22%). In terms of number of OTUs, small differences were observed among these three groups (Fig. 3). The substrate composition showed a mix of sandy and detritic sediments in GMV, with also mixed assemblages dominated by Cnidaria and followed by Porifera (Fig. 3). Cnidarians were much more abundant than any other taxonomic group in GMV (1578 individuals/colonies, Table 2), representing up to 72% of the organisms found. However, up to 70% of these records corresponded to *A. richardi,* which occurred over extensive sandy areas. Note that most of the samples (i.e., still images) of GMV were collected in the boundary of the NACW and the MOW between 400 and 500 m depth (Fig. 3). In contrast, mixed areas with sandy bottoms and outcrop rocks were observed in the two Atlantic seamounts (Fig. 3). In both, OS and FS, a clear pattern in the occurrence of taxonomic groups was observed in the depth gradient, changing from assemblages dominated by Porifera in the intermediate waters, to assemblages dominated by Cnidaria in terms of number of OTUs and abundance in the deeper waters (Fig. 3). Porifera strongly overtook in terms of abundance (88% with a total of 1591 individuals/colonies) in OS, mainly occurring in the MOW depth range (Fig. 3). The highest number of OTUs (126) and organisms (7200 individuals/colonies) were recorded in FS (Fig. 3), with a particular high diversity of Cnidaria, specifically gorgonians. However, in total, Porifera occurred in FS in larger numbers (4134 individuals/colonies) than Cnidaria (2785 individuals/colonies). The fauna explored in FS covered the largest continuous bathymetrical range (500–1600 m depth) sampled, which includes three different water masses (AAIW, MOW and NADW; Fig. 3).

3.2. Influence of substrate and water masses in the assemblage structure

The application of the aforementioned dimension reduction techniques showed the best assemblage structure analyses (based on stress or explained variability values) were obtained by applying PCO in SdO and GMV (Supp. 3), due to their smaller sample size and, nMDS with three dimensions in the case of OS and FS (Fig. 4, Supp. 3). The structure of the assemblages was mainly influenced by substrate type in SdO, GMV and OS (Supp.3), while water masses only displayed significant effects in the assemblage structure of FS (Fig. 4). In SdO most of the samples (i.e., still images) were located in areas under the influence of the LIW, which originates the MOW and therefore, the community structure was mainly defined in the PCoA by substrate type; presenting two well differentiated assemblages. Muddy substrates were dominated by fish, echinoderm, sea-pen and black coral OTUs; while the detritic bottoms were dominated by sponges and few Cnidaria OTUs (Supp.3A). In GMV the bathymetric range sampled was narrow (as it is the smallest seafloor elevation of this study) and most of the samples (i.e., still images) were taken in the range of the MOW. The samples or locations bathed by the NACW and the MOW were not strongly grouped but can be clearly differentiated in the PCoA, coinciding with two main substrate types (Supp. 3B). Samples on the MOW range were dominated by sand and strongly associated with the hormathiid actiniaria *A. richardi* and the solitary coral *Flabellum chunii*. In contrast, the locations influenced by the NACW presented mainly detritic substrates inhabited by Porifera OTUs and the cold-water scleractinian coral *Madrepora oculata*. The rest of the Cnidaria OTUs did not show clear patterns. Similar results were observed in the nMDS performed for OS since, probably, most of the samples were also collected at the MOW depth range (Supp.3C). A large number of samples cluster in a group characterized by the dominance of rocky substrates and Porifera OTUs, except for glass sponges, which occurred in a different group of samples associated with high percentages of sand. Mixed substrates of sand and detritic sediments with a strong presence of Cnidaria OTUs occurred in the NADW range (Supp.3C; at coordinates PCO1 = 0, PCO2 = 0).

In contrast, the megabenthic fauna of FS was sampled across a wide bathymetrical range, including the four main water masses (NACW, AAIW, MOW, NADW) bathing this seamount (Fig. 4). The presence of

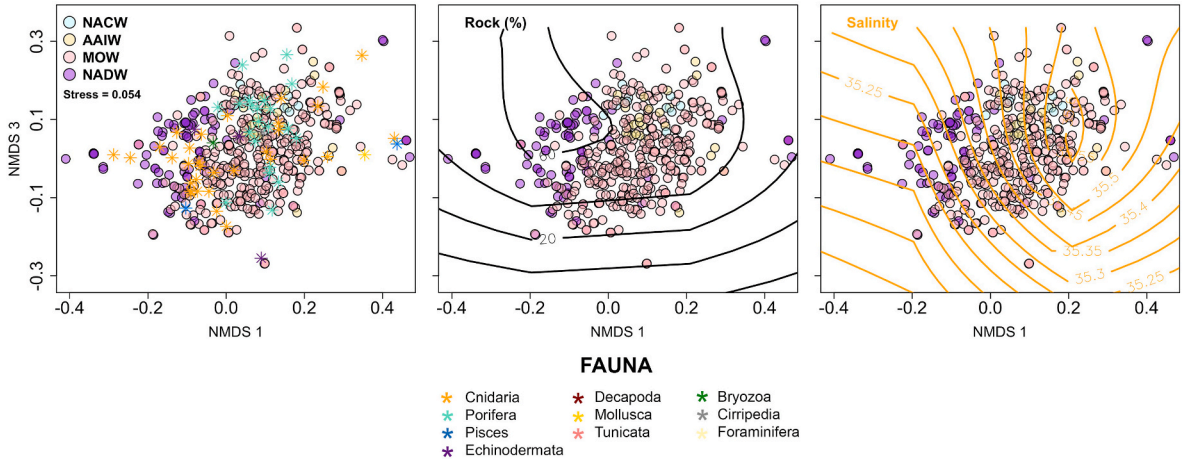

Fig. 4. Ordination biplots derived from non-Metric Multidimensional Scaling analyses in Formigas seamount. Stress values (Stress; i.e., goodness of fit) is indicated in the plot area. All axes are unitless. Samples (i.e., still images) are represented by circles colored according to the water mass identified at the location were the sample was taken. Asterisks shown the ordination of the Operational Taxonomic Units (OTUs) colored according to the main taxonomic group. Central and right plots only display samples with overlapping contour lines of the main significant ($p < 0.05$) environmental factors fitted to the assemblage ordination axis using Generalized Additive Models. Numbers in-between contour lines indicate the values of the corresponding environmental variable.

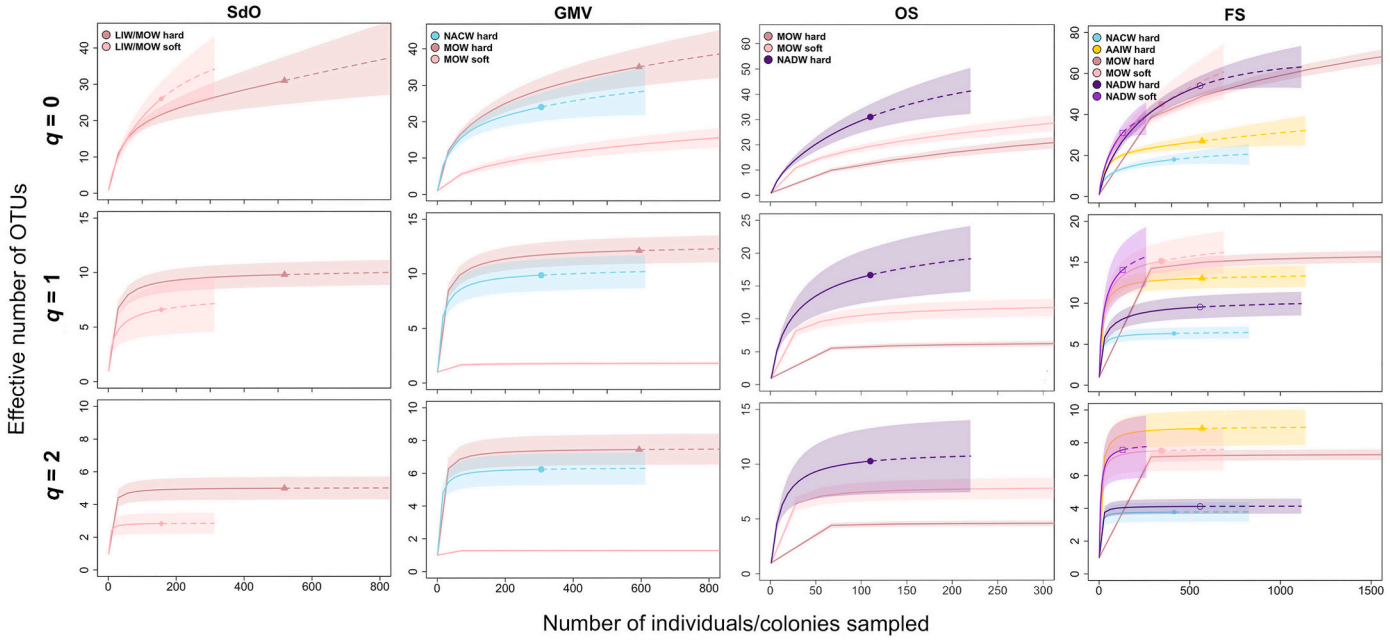

Fig. 5. Diversity measurements based on Hill numbers displayed as rarefaction/extrapolation curves for assemblage categories (water mass and substrate type) observed at the studied seafloor elevations. Solid lines denote observations and interpolated values (rarefaction), while dashed lines indicate extrapolated values. The order *q* of the Hill numbers is equivalent to richness (q = 0), Shannon (q = 1) and inverse Simpson diversity indices. Abbreviations: (OTUs) Operational Taxonomic Units. Seco de los Olivos (SdO) bank, Gazul mud volcano (GMV), Ormonde seamount (OS) and Formigas seamount. North Atlantic Central Water (NACW), Mediterranean Outflow Water (MOW) and North Atlantic Deep Water (NADW). Substrates are indicated with hard (i.e., rock, hard-flagstone and detritic) and soft (i.e, mud, sand, soft-flagstone, sandy gravels and pebbles) categories, respectively.

Table 3
Partitioning diversity (alpha, beta, gamma) and similarity indices derived from Hill numbers for assemblages based on water masses and substrate type within each studied seafloor elevation. The order *q* of the Hill numbers is equivalent to richness (q = 0), Shannon (q = 1) and inverse Simpson diversity (q = 2) indices. N denote the total number of assemblages based on water mass and substrate type combination observed (see also Fig. 5), local similarity (local) showed the proportion of shared diversity, while regional similarity (regional) displays proportion of total diversity contained on average sample.

N	q	alpha	beta	gamma	local	regional
Seco de los Olivos Bank						
2	0	28.5	1.51	43	0.49	0.32
	1	8.04	1.60	12.89	0.32	0.32
	2	3.62	1.85	6.69	0.08	0.15
Gazul mud volcano						
3	0	25.67	1.56	40	0.72	0.46
	1	6	1.92	11.56	0.40	0.40
	2	2.78	2.54	7.08	0.09	0.23
Ormonde Seamount						
3	0	34.33	2.01	69	0.49	0.25
	1	11.03	2.07	22.86	0.34	0.34
	2	6.85	2.07	14.20	0.22	0.46
Formigas Seamount						
6	0	45.83	2.75	126	0.65	0.24
	1	11.73	2.19	25.76	0.56	0.56
	2	5.80	2.25	13.05	0.33	0.75

rocky substrate together with the salinity gradient mainly defined the composition and structure of megabenthic assemblages in this seamount. Indeed, different groups of fauna clearly clustered at different water masses (Fig. 4). Cnidaria OTUs such as scleractinians and antipatharians were associated with the presence of rocky bottoms; being mostly distributed in the NADW and at the boundary of this water mass with the MOW. All the Porifera OTUs occurred in the MOW range, although the core of this water mass was dominated by Cnidaria, specifically gorgonians, and particularly the ones belonging to the genus *Narella*. Indeed, the highest salinity values clearly matched the distribution of *N. bellissima* and *N. versluysi* (at approximately coordinates NMDS1 = 0.25, NMDS3 = 0.15). A very similar pattern was also observed for temperature and dissolved oxygen, since these three variables were highly correlated ($R^2 = |0.82–0.96|$, $p < 0.05$) and form the signature of the MOW.

3.3. Diversity measurements

Overall, diversity measurements based on Hill numbers showed that the hard substrate category displayed higher richness values (q = 0) than the soft category, within a given water mass (Fig. 5). The only exception was found for the soft bottoms of OS bathed by the MOW; whose diversity was slightly higher than that found in hard substrates under this same water mass (Fig. 5). The same patterns were also observed for other diversity measurements (q = 1 and q = 2), which also considered the abundance of the OTUs, except in the case of FS; where soft bottoms seemed to host similar abundance of organisms than the hard substrates (Fig. 5). Across the four different seafloor elevations, the FS showed the highest values of diversity measurements. Note that confidence intervals of the R/E curves tended to overlap among the different assemblage categories, indicating that the average values of R/E curves were not statically different in many cases and therefore, the diversity in these categories were similar. Indeed, the partitioning diversity (Table 3) showed similar results and patterns.

In SdO, the two assemblage categories observed (i.e., LIW/MOW hard and LIW/MOW soft) did not completely display a clear differentiation in terms of diversity measurements q = 0 and q = 1, as indicated by beta diversity values lower than 2 (i.e., two effective differentiated

assemblages) and high (>0.30; i.e., similarity larger than 30%) similarity indices (Table 3). Similar results were detected for the three assemblage categories in GMV (Table 3), where the diversity between Atlantic and Mediterranean waters seemed to be similar (Fig. 5). Indeed, the pairwise comparisons of all the assemblage categories at GMV (Supp. 3) confirmed that the main differences among them were due to different substrate types. Despite of the high similarity values observed in OS, partitioning diversity analyses identified two differentiated assemblages (Table 3) from the 3 assemblage categories compared (Fig. 5). In this case, the pairwise comparisons showed much larger differences between the MOW and the NADW assemblages than those among different substrate types within the MOW (Supp. 3). Finally, among the six assemblage categories compared in FS, the differentiated assemblages found by the partitioning diversity analyses varied between 2 and 3 depending on the diversity index considered (Table 3). In terms of species richness ($q = 0$), the pairwise comparisons showed larger differences among the water masses NACW, NADW and MOW; than among different substrate types within each of these water masses (Supp.3). However, when consider the other two diversity measurements ($q = 1$ and $q = 2$), the largest differences were observed between hard bottom assemblages under the NACW influence and those of soft bottoms under the NADW influence (Supp. 3).

4. Discussion

The results obtained from the MEDWAVES expedition provide, for the first time, a large-scale quantitative characterization of the deep-sea megabenthic assemblages along the western branch of the MOW, from its origin in the western Mediterranean Sea to the Central North Atlantic at the Azores Islands. In the present study, we inventoried almost 12,000 organisms from deep-sea megabenthic fauna belonging to 216 Operational Taxonomic Units (OTUs). Despite of the large identification efforts supported by expert taxonomists, only 75 OTUs were identifiable to the species and 31 to the genus levels, while many remain identified as morphotypes at high taxonomic levels (Table 2). This is a common issue in studies using underwater images, especially in deep-sea areas where current taxonomic knowledge is still a challenge, even when samples are available (Henry and Roberts, 2014; Howell et al., 2019). For some of the studied areas, such as Ormonde (OS) and Formigas (FS) seamounts, these are the first quantitative data reported for deep-sea megabenthic fauna. Several of these inventoried OTUs are habitat-forming species such as cold-water corals (CWCs), gorgonians or sponges, which dominated the four studied seafloor elevations in terms of abundance and further shaped and characterized the benthic assemblages and habitats. As such, most of these OTUs (e.g., aggregations of *Lophelia pertusa*, *Madrepora oculata*, Porifera massive, etc.) have been identified as key indicators of deep-sea Vulnerable Marine Ecosystems (VME; UNGA, 2006) due to their rarity, fragility, low recovery potential and critical significance for the ecosystem functioning. In this sense, the states and the regional fisheries management organizations are bound to prevent adverse impacts on such ecosystems, particularly those derived from fishing activities causing disturbance of the seabed (FAO, 2009; ICES, 2017). We presented the patterns in assemblage composition, structure and biodiversity at local scale (i.e., at each seafloor elevation) in order to better understand and disentangle the influence of substrate type and water masses on deep-sea megafauna in different types of seafloor elevations.

4.1. Substrate vs water mass influence on the composition and structure of megabenthic assemblages

There is a comprehensive knowledge regarding the importance of substrate modulating the occurrence of some benthic species, with a clear differentiation between broad categories of soft and hard bottoms (e.g. Howell et al., 2010). Additionally, and particularly for benthic fauna at seafloor elevations (Clark et al., 2010; Rogers, 2018), depth has been also pointed as one of the main drivers defining a clear faunal zonation in the structure of these assemblages (Clark et al., 2010; McClain and Lundsten, 2015; Du Preez et al., 2016). However, depth generally reflects (and correlates with) other environmental gradients such as temperature, oxygen concentration, food availability, etc., which are mainly defined by the water mass structure (Liu and Tanhua, 2019; Puerta et al., 2020 and references therein). Therefore, this vertical distribution of some benthic species and assemblages is likely not to be a direct consequence of the depth gradient itself. Indeed, recent studies acknowledge the importance of water masses in shaping biodiversity and structure of some deep-sea benthic communities, since their properties better enclose and track the environmental gradients at different spatio-temporal scales (see Puerta et al., 2020 for a review). However, to our best knowledge, only a few studies (Arantes et al., 2009; Auscavitch et al., 2020; Radice et al., 2016; Roberts et al., 2021; Somoza et al., 2021; Victorero et al., 2018) directly investigated the effect of water masses shaping observed patterns in deep-sea benthic assemblages, habitats or ecosystems.

Here, we compared the effects of substrate type and water masses (considered as particular combination of different physico-chemical variables) on the deep-sea benthic assemblages through large environmental gradients and over an extensive spatial scale. The results indicate a strong effect of the main substrate type on the structure and diversity of the assemblages in all the studied seafloor elevations, with hard-bottom and soft-bottom assemblages clearly differentiated in benthic megafauna composition and structure. However, the oceanographic structure (water masses found at different depths) also played a potential role in structuring some of these deep-sea megabenthic assemblages, in agreement with other studies (Arantes et al., 2009; Auscavitch et al., 2020; Radice et al., 2016; Victorero et al., 2018). For example, in large seafloor elevations with a large bathymetrical range that encompasses several water masses (e.g., OS and FS; see Mosquera-Giménez et al., 2019 for details on different the water masses), the influence of these water masses on the assemblage structure and diversity become much clearer and stronger and sometimes might even explain more variability than the differences in substrate types. Thus, for example, the assemblages bathed by the Atlantic (NACW, NADW) and Mediterranean (MOW) waters tended to be clearly differentiated at OS and FS in terms of species richness and abundance regardless the substrate. In particular, the presence of the MOW at FS seemed to have a notable effect on assemblage structuring and diversity, since the largest abundance of benthic suspension feeders were observed in this seamount at the MOW interface (~700m depth) as already documented by (Mosquera-Giménez et al., 2019). However, this water mass was sampled more intensively and therefore, these results should be taken cautiously (see more details below). On the contrary, small seafloor elevations such as Gazul mud volcano (GMV) did not display strong differences regarding water masses, being substrate type the main modulating variable influencing the occurrence of different assemblages as already detected in a previous study (Urra et al., 2021).

The stratification (e.g., Lavelle and Mohn, 2010; Mienis et al., 2007; White and Dorschel, 2010) and/or strong gradients (Mosquera-Giménez et al., 2019) in the structure of water masses have been reported to occur in multiple seamounts of the North Atlantic, including GMV, OS and FS (Mosquera-Giménez et al., 2019). This stratification at depth leads to internal wave motions, which interact with the slope of the seamounts, can end up breaking, and therefore, enhancing the vertical mixing and material resuspension. These local oceanographic effects may turn seamounts into very productive ecosystems with high food availability that enhances the presence of benthic organisms (e.g., Lavelle and Mohn, 2010; Mosquera-Giménez et al., 2019). However, it is likely that the individual variables that characterize the water masses and/or other oceanographic such as, current velocities, carbonate chemistry, nutrient concentration or oxygen values, among others, also played a relevant role defining the structure and diversity of the deep-sea megabenthic assemblages (Puerta et al., 2020; Rogers, 2018) and their effects need to

be disentangle in further studies.

4.2. Large-scale role of the MOW in biodiversity patterns

Water masses contribute to drive the dispersal of species and connectivity among distant ecosystems, including those in the deep-sea (Cowen and Sponaugle, 2009; Gary et al., 2020; Henry et al., 2014; Hilário et al., 2015; Metaxas et al., 2019), being crucial for survival, growth, spread, recovery from damage and adaptation to changing condition in space and time (Cowen and Sponaugle, 2009; Hebbeln et al., 2019; Metaxas et al., 2019). Although further research is still required, the MOW seems to be a key dispersal pathway in the deep North Atlantic (Gary et al., 2020; Hebbeln et al., 2019; Henry et al., 2014) influencing the distribution and connectivity patterns and linking Mediterranean and Atlantic species and populations of deep-sea fauna, including CWCs (Arnaud-Haond et al., 2017; Boavida et al., 2019; Dullo et al., 2008; Henry et al., 2014; Somoza et al., 2014) and sponges (Palomino et al., 2016; Sitjá et al., 2018; Sitjà et al., 2020). In agreement with those and other previous studies (Puerta et al., 2020; Somoza et al., 2021), our results also pointed the potential role of the MOW for biodiversity and biogeographic patterns at the North Atlantic basin. Indeed, our results indicated that the MOW, among the different water masses studied, and FS, among the different studied seafloor elevations, presented the largest diversity values. However, these conclusions regarding the role of the MOW should be taken very cautiously due to the particular characteristics of the data collection used. First, the obtained sample size was largely unbalanced among both, water masses (NACW = 86, MOW = 1920, NADW = 456 still images) and the studied seafloor elevations (SdO = 489, GMV = 355, OS = 615, FS = 1029 still images). This situation derived from the main objectives of the MEDWAVES expedition (Orejas et al., 2017), which particularly targeted areas under the influence of the MOW and the less explored seamounts (FS and OS). Despite of the use of Hill numbers to counterbalance the differences on sample size (Chao et al., 2014a), to our best judgement, the results may still show some bias due to sampling design since R/E curves did not achieve a steady (constant) shape in all cases (Fig. 5). Secondly, the different impacts of the anthropogenic activities (mainly fisheries) and the different times and levels of protection could also generate further differences across the studied seafloor elevations. The SdO and GMV have been traditionally subjected to intense multi-gear fishing activities, led mainly by trawling (de la Torriente et al., 2014; González-García et al., 2020; Urra et al., 2021), the most damaging fishing technique for benthic ecosystems (Clark et al., 2016; Pusceddu et al., 2014). In contrast, longlines have been traditionally the most common fishery in OS (Vieira et al., 2015) and the Azores area (Pham et al., 2013). However, fishing activity in the OS region was practically abandoned in 2012 (Vieira et al., 2015), while FS was declared an offshore marine reserve in 1988 (Martins and Santos, 1988) following strong restrictions in fisheries since then (Santos et al., 1995). Therefore, differences in assemblage diversity observed across the studied areas may not be only derived from the particular environmental characteristics. At the local scale (i.e., at each individual seafloor elevation), the assemblages bathed by the MOW were in all cases among the most diverse ones in terms of both, species richness and abundance, suggesting the existence of potential role of the MOW at larger scale to favor biodiversity of deep-sea megabenthic fauna. However, the aforementioned issues with sampling design cannot be discarded either. Despite of previous studies of the deep-sea fauna of the Azores showed considerable Mediterranean affinities in species composition (Braga-Henriques et al., 2013; Sampaio et al., 2019), just a few of these species were found within the bathymetric range studied in FS. These Mediterranean affinities seem to be mainly associated with the presence of some shared CWC species (Braga-Henriques et al., 2013; Sampaio et al., 2019), while very small Mediterranean affinities have been identified for deep-sea sponges (Sitjà et al., 2020). For instance, the distribution patterns of the CWC *Madrepora oculata* seemed to follow the vertical distribution of the MOW across the different seafloor elevations ranging from 240 to 300 m in SdO (4 colonies), 400–465 m in GMV (98 colonies) and 1180–1215 m in FS (18 colonies; Table 2).

Multiple works address the natural export of fish and benthic fauna from the surface Atlantic waters into the Mediterranean Sea through the Strait of Gibraltar (Ben Rais Lasram et al., 2008; Pérès, 1985; Pérès and Piccard, 1964; Templado et al., 1986, 2006). Dispersion of benthic species in the opposite direction also seem to occur at deep waters, but this has been less investigated and it is thought to be a much lower intense process (Sitjà et al., 2019, 2020), mainly acting at geological time scales (Boavida et al., 2019; Henry et al., 2014). Some studies reported the presence of deep-sea benthic species previously known only from the Mediterranean Sea in the Gulf of Cádiz, such as deep-sea sponges (Sitjà et al., 2019, 2020), bryozoans (Harmeling et al., 1993), ascidians (Monniot and Monniot, 1988), crinoids (Palomino et al., 2016) and hydroids (Henry and Roberts, 2008) in the British Islands; supporting the existence of a more contemporary transfer of deep-sea species. However, how far the current MOW export can reach or why it appears to be more effective for some taxonomic groups than others still remain unclear (Sitjà et al., 2020). The physical characteristics of the MOW, such as warmer temperature for instance, have been hypothesized to positively affect the development of CWC communities at distant locations (De Mol et al., 2005; Dodds et al., 2007; Sánchez et al., 2014; Van Rooij et al., 2010). However, other factors and processes associated to the circulation of main water masses such as enhancement of food availability, larval dispersion or retention, etc. (Puerta et al., 2020; Roberts et al., 2021) cannot be discarded and need further investigation.

5. Conclusions

Water masses not only exert control over the connectivity and biogeographic patterns at large spatio-temporal scales, but can also locally influence the environmental conditions shaping the structure of some deep-sea megabenthic communities. Biodiversity analyses could differentiate the assemblages under the influence of Mediterranean and the Atlantic waters in presence of large bathymetrical range. The relative importance of local versus historical (Hebbeln et al., 2019; Henry et al., 2014) processes related to water masses in shaping deep-sea biogeographic patterns is still scarcely understood, but seemed to play a crucial role for other marine organisms e.g. (Bonecker et al., 2019; Djurhuus et al., 2017; Hernando-Morales et al., 2017). Understanding water masses as an integrative tool to delineate biodiversity and biogeographic patterns (Puerta et al., 2020) will be key to identify deep-sea vulnerable ecosystems and regions of refugia under future climate change conditions.

Author contributions

PP, CO, MC-S and CDC designed the concept of the study, PP designed the structure, coordinate and primarily wrote the manuscript. CO designed and led the oceanographic expedition. TM contributed to select some of the study areas of the expedition. CO, JLR, JU, CG-Z, YS, PV-B, MC-S and JR gathered data during the oceanographic expedition. AM-G and PV-B compile and processed the oceanographic data on water masses and JR bathymetric data. CDC, YS, PP, TM and OR designed the video and still image analysis protocol. CDC, YS, JB-F, JU, PP, OR, CG-Z performed the still image analyses. PP designed and performed the statistical analyses. All authors were substantially involved in the taxonomic identification, literature search and/or writing of the different sections of the manuscript, contributed to the final product in significant ways, and provided approval for publication.

Declaration of competing interest

The authors declare that they have no known competing financial

interests or personal relationships that could have appeared to influence the work reported in this paper.

Acknowledgements

We would like to thank Álvaro Altuna (Museo de Okendo), Ricardo Aguilar (OCEANA), Georgios Kazanidis (University of Edinburgh), Lais Vieira Ramalho (UFRJ), Iris Sampaio, Valentina Matos Filipe Porteiro and Manuela Ramos (IMAR) for their help with the taxonomic identification and the processing of some samples. We also thank the research group Geociencias Marinas from IEO for providing bathymetry data of GMV from the project LIFE + INDEMARES CHICA for the ROV sampling design of Gazul mud volcano during the MEDWAVES expedition and Gerardo Bruque (IEO) for his help with mapping and figures. The MEDWAVES expedition was supported by the ATLAS project and the Spanish Ministry of Economy, Industry and Competitivity. We are grateful to the captain and all the crew of the RV Sarmiento de Gamboa, the Marine Technology Unit (UTM – CSIC), the ROV team from ACSM and the MEDWAVES scientific party.

This study has received funding from the European Union's Horizon 2020 research and innovation program under the projects, grant agreement No 678760 (ATLAS) and 818123 (iAtlantic). This output reflects only the author's view and the European Union cannot be held responsible for any use that may be made of the information contained therein. M.C.S., C.D.-C., J.B.-F. and T.M. also acknowledge funds and support from the FCT through the strategic pro-ject (UIDB/05634/2020 and UIDP/05634/2020) granted to OKEANOS and through the FCT Regional Government of the Azores under the project M1.1.A/REEQ. CIENTÍFICO UI&D/2021/010. C.D.-C. was supported by the PO2020 project DeepWalls (s) and by the FCT-IP Pro-ject UIDP/05634/2020. M. C.S. and T.M. were supported by Program Stimulus of Scientific Employment (CCCIND/03346/2020 and CCCIND/03345/2020, respectively) from the Fundação para a Ciência e Tec-nologia.

References

Abdel-Monem, A.A., Fernandez, L.A., Boone, G.M., 1975. K-Ar ages from the eastern azores group (santa maria, são miguel and the Formigas islands). Lithos 8, 247–254. https://doi.org/10.1016/0024-4937(75)90008-0.

Addamo, A.M., Vertino, A., Stolarski, J., Garcia-Jimenez, R., Taviani, M., Machordom, A., 2016. Merging scleractinian genera: the overwhelming genetic similarity between solitary Desmophyllum and colonial Lophelia. BMC Evol. Biol. 16, 108. https://doi.org/10.1186/s12862-016-0654-8.

Arantes, R.C.M., Castro, C.B., Pires, D.O., Seoane, J.C.S., 2009. Depth and water mass zonation and species associations of cold-water octocoral and stony coral communities in the southwestern Atlantic. Mar. Ecol. Prog. Ser. 397, 71–79. https://doi.org/10.3354/meps08230.

Arnaud-Haond, S., Van den Beld, I.M.J., Becheler, R., Orejas, C., Menot, L., Frank, N., Grehan, A., Bourillet, J.F., 2017. Two "pillars" of cold-water coral reefs along Atlantic European margins: prevalent association of *Madrepora oculata* with *Lophelia pertusa*, from reef to colony scale. Deep. Res. Part II Top. Stud. Oceanogr. 145, 110–119. https://doi.org/10.1016/j.dsr2.2015.07.013.

Auscavitch, S.R., Deere, M.C., Keller, A.G., Rotjan, R.D., Shank, T.M., Cordes, E.E., 2020. Oceanographic drivers of deep-sea coral species distribution and community assembly on seamounts, islands, atolls, and reefs within the phoenix islands protected area. Front. Mar. Sci. 7, 1–15. https://doi.org/10.3389/fmars.2020.00042.

Bashmachnikov, I., Nascimento, Â., Neves, F., Menezes, T., Koldunov, N.V., 2015. Distribution of intermediate water masses in the subtropical northeast Atlantic. Ocean Sci. 11, 803–827. https://doi.org/10.5194/os-11-803-2015.

Ben Rais Lasram, F., Tomasini, J.A., Romdhane, M.S., Do Chi, T., Mouillot, D., 2008. Historical colonization of the Mediterranean Sea by Atlantic fishes: do biological traits matter? Hydrobiologia 607, 51–62. https://doi.org/10.1007/s10750-008-9366-4.

Berglund, S., Döös, K., Nycander, J., 2017. Lagrangian tracing of the water–mass transformations in the Atlantic Ocean. Tellus Dyn. Meteorol. Oceanogr. 69, 1306311 https://doi.org/10.1080/16000870.2017.1306311.

Bo, M., Bertolino, M., Borghini, M., Castellano, M., Harriague, A.C., Di Camillo, C.G., Gasparini, G., Misic, C., Povero, P., Pusceddu, A., Schroeder, K., Bavestrello, G., 2011. Characteristics of the mesophotic megabenthic assemblages of the vercelli seamount (north tyrrhenian sea). PLoS One 6. https://doi.org/10.1371/journal.pone.0016357.

Boavida, J.R.H., Becheler, R., Choquet, M., Frank, N., Taviani, M., Bourillet, J.-F.F., Meistertzheim, A.L., Grehan, A., Savini, A., Arnaud-Haond, S., 2019. Out of the Mediterranean? Post-glacial colonization pathways varied among cold-water coral species. J. Biogeogr. 46, 915–931. https://doi.org/10.1111/jbi.13570.

Bonecker, A.C.T., Dias, C.D.O., De Castro, M.S., De Carvalho, P.F., Araujo, A.V., Paranhos, R., Cabral, A.S., Bonecker, S.L.C., 2019. Vertical distribution of mesozooplankton and ichthyoplankton communities in the South-western Atlantic Ocean (23°14′1″S 40°42′19″W). J. Mar. Biol. Assoc. U. K. 99, 51–65. https://doi.org/10.1017/S0025315417001989.

Bozec, A., Lozier, M.S., Chassignet, E.P., Halliwell, G.R., 2011. On the variability of the mediterranean outflow water in the north atlantic from 1948 to 2006. J. Geophys. Res. Ocean. 116 https://doi.org/10.1029/2011JC007191.

Braga-Henriques, A., Porteiro, F.M., Ribeiro, P.A., De Matos, V., Sampaio, Í., Ocaña, O., Santos, R.S., de Matos, V., Sampaio, Í., Ocaña, O., Santos, R.S., De Matos, V., Sampaio, Í., Ocaña, O., Santos, R.S., 2013. Diversity, distribution and spatial structure of the cold-water coral fauna of the Azores (NE Atlantic). Biogeosciences 10, 4009–4036. https://doi.org/10.5194/bg-10-4009-2013.

Breusing, C., Biastoch, A., Drews, A., Metaxas, A., Jollivet, D., Vrijenhoek, R.C., Bayer, T., Melzner, F., Sayavedra, L., Petersen, J.M., Dubilier, N., Schilhabel, M.B., Rosenstiel, P., Reusch, T.B.H., 2016. Biophysical and population genetic models predict the presence of "phantom" stepping stones connecting Mid-Atlantic Ridge vent ecosystems. Curr. Biol. 26, 2257–2267. https://doi.org/10.1016/j.cub.2016.06.062.

Candela, J., 2001. Mediterranean water and global circulation. In: Sedler, G., Church, J., Gould, J. (Eds.), Ocean Circulation and Climate Observing and Modelling the Global Ocean. Int. Geophys, 77, pp. 419–XLVIII.

Carney, R.S., 2005. Zonation of deep biota on continental margins. Oceanogr. Mar. Biol. 43, 211–278.

Chao, A., Chiu, C.H., Jost, L., 2014a. Unifying species diversity, phylogenetic diversity, functional diversity, and related similarity and differentiation measures through hill numbers. Annu. Rev. Ecol. Evol. Syst. 45, 297–324. https://doi.org/10.1146/annurev-ecolsys-120213-091540.

Chao, A., Gotelli, N.J., Hsieh, T.C., Sander, E.L., Ma, K.H., Colwell, R.K., Ellison, A.M., 2014b. Rarefaction and extrapolation with Hill numbers: a framework for sampling and estimation in species diversity studies. Ecol. Monogr. 84, 45–67. https://doi.org/10.1890/13-0133.1.

Clark, M.R., Althaus, F., Schlacher, T.A., Williams, A., Bowden, D.A., Rowden, A.A., 2016. The impacts of deep-sea fisheries on benthic communities: a review. ICES J. Mar. Sci. 73, i51–i69. https://doi.org/10.1093/icesjms/fsv123.

Clark, M.R., Rowden, A.A., Schlacher, T., Williams, A., Consalvey, M., Stocks, K.I., Rogers, A.D., O'Hara, T.D., White, M., Shank, T.M., Hall-Spencer, J.M., 2010. The ecology of seamounts: structure, function, and human impacts. Ann. Rev. Mar. Sci 2, 253–278. https://doi.org/10.1146/annurev-marine-120308-081109.

Cowen, R.K., Sponaugle, S., 2009. Larval dispersal and marine population connectivity. Ann. Rev. Mar. Sci 1, 443–466. https://doi.org/10.1146/annurev.marine.010908.163757.

Cuny, J., Rhines, P.B., Niiler, P.P., Bacon, S., 2002. Labrador sea boundary currents and the fate of the irminger sea water. J. Phys. Oceanogr. 32, 627–647. https://doi.org/10.1175/1520-0485(2002)032<0627:LSBCAT>2.0.CO;2.

Daniault, N., Mazé, J.P., Arhan, M., 1994. Circulation and mixing of mediterranean water west of the iberian peninsula. Deep-Sea Res. Part I Oceanogr. Res. Pap. 41, 1685–1714. https://doi.org/10.1016/0967-0637(94)90068-X.

de la Torriente, A., Aguilar, R., Serrano, A., García, S., Fernández, L.M., García Muñoz, M., Punzón, A., Arcos, J.M., Sagarminaga, R., 2014. Sur de Almería - Seco de los Olivos. Proyecto LIFE+ INDEMARES.

de la Torriente, A., González-Irusta, J.M., Aguilar, R., Fernández-Salas, L.M., Punzón, A., Serrano, A., 2019. Benthic habitat modelling and mapping as a conservation tool for marine protected areas: a seamount in the western Mediterranean. Aquat. Conserv. Mar. Freshw. Ecosyst. 29, 732–750. https://doi.org/10.1002/aqc.3075.

De Mol, B., Amblas, D., Calafat, A., Canals, M., Duran, R., Lavoie, C., Muñoz, A., Rivera, J., 2012. Cold-water coral colonization of Alboran Sea knolls, western Mediterranean Sea. In: Harris, P.T., Baker, E.K. (Eds.), Seafloor Geomorphology as Benthic Habitat. Elsevier, London, pp. 819–829. https://doi.org/10.1016/B978-0-12-385140-6.00060-8.

De Mol, B., Henriet, J.-P., Canals, M., 2005. Development of coral banks in Porcupine Seabight: do they have Mediterranean ancestors? In: Freiwald, A., Roberts, J.M. (Eds.), Cold-Water Corals and Ecosystems. Springer, Berlin Heidelberg, pp. 515–533. https://doi.org/10.1007/3-540-27673-4_26.

de Pascual-Collar, Á., Sotillo, M.G., Levier, B., Aznar, R., Lorente, P., Amo-Baladrón, A., Álvarez-Fanjul, E., 2019. Regional circulation patterns of mediterranean outflow water near the iberian and african continental slopes. Ocean Sci. 15, 565–582. https://doi.org/10.5194/os-15-565-2019.

Djurhuus, A., Boersch-Supan, P.H., Mikalsen, S.-O., Rogers, A.D., 2017. Microbe biogeography tracks water masses in a dynamic oceanic frontal system. R. Soc. Open Sci. 4, 170033 https://doi.org/10.1098/rsos.170033.

Dodds, L.A., Roberts, J.M., Taylor, A.C., Marubini, F., 2007. Metabolic tolerance of the cold-water coral Lophelia pertusa (Scleractinia) to temperature and dissolved oxygen change. J. Exp. Mar. Biol. Ecol. 349, 205–214. https://doi.org/10.1016/j.jembe.2007.05.013.

Dullo, W.C., Flogel, S., Ruggeberg, A., Flögel, S., Rüggeberg, A., 2008. Cold-water coral growth in relation to the hydrography of the Celtic and Nordic European continental margin. Mar. Ecol. Prog. Ser. 371, 165–176. https://doi.org/10.3354/meps07623.

Du Preez, C. Du, Curtis, J.M.R., Clarke, M.E., 2016. The structure and distribution of benthic communities on a shallow seamount (Cobb Seamount, Northeast Pacific Ocean). PLoS One 11, 1–29. https://doi.org/10.1371/journal.pone.0165513.

Emery, W.J., 2015. Oceanographic topics: water types and water masses. Encycl. Atmos. Sci. 329–337. https://doi.org/10.1016/B978-0-12-382225-3.00279-6 second ed.

Etter, R.J., Bower, A.S., 2015. Dispersal and population connectivity in the deep North Atlantic estimated from physical transport processes. Deep. Res. Part I Oceanogr. Res. 104, 159–172. https://doi.org/10.1016/j.dsr.2015.06.009.
FAO. International guidelines for the management of deep-sea fisheries in the high seas directives. Food and Agricultural Organization of the United Nations. http://www.fao.org/3/i0816t/I0816T.pdf.
Ferranti, L., Passaro, S., de Alteriis, G., 2014. Morphotectonics of the Gorringe Bank summit, eastern Atlantic Ocean, based on high-resolution multibeam bathymetry. Quat. Int. 332, 99–114. https://doi.org/10.1016/j.quaint.2013.11.011.
Fox, A.D., Henry, L.-A., Corne, D.W., Roberts, J.M., 2016. Sensitivity of marine protected area network connectivity to atmospheric variability. R. Soc. Open Sci. 3, 160494 https://doi.org/10.1098/rsos.160494.
Fuhr, M., Laukert, G., Yu, Y., Nürnberg, D., Frank, M., 2021. Tracing water mass mixing from the equatorial to the north pacific ocean with dissolved neodymium isotopes and concentrations. Front. Mar. Sci. 7, 603761.
García-Ibáñez, M.I., Pardo, P.C., Carracedo, L.I., Mercier, H., Lherminier, P., Ríos, A.F., Pérez, F.F., 2015. Structure, transports and transformations of the water masses in the Atlantic Subpolar Gyre. Prog. Oceanogr. 135, 18–36. https://doi.org/10.1016/j.pocean.2015.03.009.
Gary, S.F., Fox, A.D., Biastoch, A., Roberts, J.M., Cunningham, S.A., 2020. Larval behaviour, dispersal and population connectivity in the deep sea. Sci. Rep. 10, 1–12. https://doi.org/10.1038/s41598-020-67503-7.
Gascard, J.C., Richez, C., 1985. Water masses and circulation in the western Alboran Sea and in the straits of Gibraltar. Prog. Oceanogr. 15, 157–216. https://doi.org/10.1016/0079-6611(85)90031-X.
González-García, E., Mateo-Ramírez, Á., Urra, J., Farias, C., García, T., Gil, J., Raso, J.E. G., López-González, N., Rueda, J.L., 2020. Bottom trawling activity, main fishery resources and associated benthic and demersal fauna in a mud volcano field of the Gulf of Cádiz (southwestern Iberian Peninsula). Reg. Stud. Mar. Sci. 33, 100985 https://doi.org/10.1016/j.rsma.2019.100985.
Groeskamp, S., Griffies, S.M., Iudicone, D., Marsh, R., Nurser, A.J.G., Zika, J.D., 2019. The water mass transformation framework for ocean physics and biogeochemistry. Ann. Rev. Mar. Sci 11, 271–305. https://doi.org/10.1146/annurev-marine-010318-095421.
Harmeling, J., Jl, D., Harmelin, J.G., D'Hondt, J.L., 1993. Transfers of bryozoan species between the Atlantic Ocean and the Mediterranean Sea via the Strait of Gibraltar. Acta Oecol. 16, 63–72.
Hebbeln, D., Portilho-Ramos, R. da C., Wienberg, C., Titschack, J., 2019. The fate of cold-water corals in a changing world: a geological perspective. Front. Mar. Sci. 6, 1–8. https://doi.org/10.3389/fmars.2019.00119.
Henry, L.-A., Roberts, J.M., 2014. Recommendations for best practice in deep-sea habitat classification: bullimore et al. as a case study. ICES J. Mar. Sci. 71, 895–898.
Henry, L.-A., Roberts, J.M., 2008. First record of *Bedotella armata* (Cnidaria: Hydrozoa) from the Porcupine Seabight: do north-east Atlantic carbonate mound fauna have Mediterranean ancestors? Mar. Biodivers. Rec. 1, e24. https://doi.org/10.1017/S1755267206002302.
Henry, L.-A., Frank, N., Hebbeln, D., Wienberg, C., Robinson, L., van de Flierdt, T., Dahl, M., Douarin, M., Morrison, C.L., Correa, M.L., Rogers, A.D., Ruckelshausen, M., Roberts, J.M., 2014. Global ocean conveyor lowers extinction risk in the deep sea. Deep. Res. Part I Oceanogr. Res. 88, 8–16. https://doi.org/10.1016/j.dsr.2014.03.004.
Hernando-Morales, V., Ameneiro, J., Teira, E., 2017. Water mass mixing shapes bacterial biogeography in a highly hydrodynamic region of the Southern Ocean. Environ. Microbiol. 19, 1017–1029. https://doi.org/10.1111/1462-2920.13538.
Hilário, A., Metaxas, A., Gaudron, S.M., Howell, K.L., Mercier, A., Mestre, N.C., Ross, R. E., Thurnherr, A.M., Young, C., 2015. Estimating dispersal distance in the deep sea: challenges and applications to marine reserves. Front. Mar. Sci. 2, 1–14. https://doi.org/10.3389/fmars.2015.00006.
Howell, K.L., 2010. A benthic classification system to aid in the implementation of marine protected area networks in the deep/high seas of the NE Atlantic. Biol. Conserv. 143, 1041–1056. https://doi.org/10.1016/j.biocon.2010.02.001.
Howell, K.L., Davies, J.S., Louise Allcock, A., Braga-Henriques, A., Buhl-Mortensen, P., Carreiro-Silva, M., Dominguez-Carrió, C., Durden, J.M., Foster, N.L., Game, C.A., Hitchin, B., Horton, T., Hosking, B., Jones, D.O.B., Mah, C., Marchais, C.L., Menot, L., Morato, T., Pearman, T.R.R., Piechaud, N., Ross, R.E., Ruhl, H.A., Saeedi, H., Stefanoudis, P.V., Taranto, G.H., Michael, B.T., Taylor, J.R., Tyler, P., Vad, J., Victorero, L., Vieira, R.P., Woodall, L.C., Xavier, J.R., Wagner, D., 2019. A framework for the development of a global standardised marine taxon reference image database (SMarTaR-ID) to support image-based analyses. bioRxiv 1–25. https://doi.org/10.1101/670786.
Howell, K.L., Davies, J.S., Narayanaswamy, B.E., 2010. Identifying deep-sea megafaunal epibenthic assemblages for use in habitat mapping and marine protected area network design. J. Mar. Biol. Assoc. U. K. 90, 33–68. https://doi.org/10.1017/S0025315409991299.
Hsieh, T.C., Ma, K.H., Chao, A., 2016. iNEXT: an R package for rarefaction and extrapolation of species diversity (Hill numbers). Methods Ecol. Evol. 7, 1451–1456. https://doi.org/10.1111/2041-210X.12613.
ICES, 2017. EU request on indicators of the pressure and impact of bottom-contacting fishing gear on the seabed, and of trade-offs in the catch and the value of landings. ICES Spec. Req. advice 1–29. Available at: https://www.ices.dk/sites/pub/Publication%20Reports/Advice/2017/Special_requests/eu.2017.13.pdf.
Iorga, M.C., Lozier, M.S., 1999. Signatures of the Mediterranean outflow from a North Atlantic climatology 1. Salinity and density fields. J. Geophys. Res. 104, 25985–26009. https://doi.org/10.1029/1999jc900115.
Jost, L., 2007. Partitioning diversity into independent alpha an beta components. Ecology 88, 2427–2439. https://doi.org/10.1890/06-1736.1.
Lacharité, M., Metaxas, A., 2017. Hard substrate in the deep ocean: how sediment features influence epibenthic megafauna on the eastern Canadian margin. Deep-Sea Res. Part I Oceanogr. Res. Pap. 126, 50–61. https://doi.org/10.1016/j.dsr.2017.05.013.
Lavelle, J.W., Mohn, C., 2010. Motion, commotion, and biophysical connections at deep ocean seamounts. Oceanography 23, 90–103. https://doi.org/10.5670/oceanog.2010.64.
Li, D., 2018. hillR: taxonomic, functional, and phylogenetic diversity and similarity through Hill Numbers. J. Open Source Softw. 3, 1041. https://doi.org/10.21105/joss.01041.
Liu, M., Tanhua, T., 2019. Characteristics of water masses in the Atlantic Ocean based on GLODAPv2 data. Ocean Sci. Discuss. https://doi.org/10.5194/os-2018-139.
Llompart, C., 1988. Braquiópodos del banco de Chella (Mar de Alborán, Mediterráneo Occidental). Acta Geol. Hisp. 23, 311–319.
Lo Iacono, C., Gràcia, E., Bartolomé, R., Coiras, E., Jose Dañobeitia, J., Acosta, J., 2012. In: Harris, P.T., Baker, E.K. (Eds.), Habitats of the Chella Bank, Eastern Alboran Sea (Western Mediterranean). Elsevier, London, pp. 681–690. https://doi.org/10.1016/B978-0-12-385140-6.00049-9.
Lo Iacono, C., Gracia, E., Diez, S., Bozzano, G., Moreno, X., Danobeitia, J., Alonso, B., 2008. Seafloor characterization and backscatter variabi lity of the Almeria Margin (Alboran Sea, SW Mediterranean) based on high-resolution acoustic data. Mar. Geol. 250, 1–18. https://doi.org/10.1016/j.margeo.2007.11.004.
Long, D.J., Baco, A.R., 2014. Rapid change with depth in megabenthic structure-forming communities of the Makapu'u deep-sea coral bed. Deep Sea Res. Part II Top. Stud. Oceanogr. 99, 158–168. https://doi.org/10.1016/j.dsr2.2013.05.032.
Marcon, Y., Purser, A., 2017. PAPARA(ZZ)I: an open-source software interface for annotating photographs of the deep-sea. Software 6, 69–80. https://doi.org/10.1016/j.softx.2017.02.002.
Martins, J., Santos, R.S., 1988. Breves considerações sobre a implementação de reservas marinhas nos Açores. In: Dias, E., Carretas, J.P., Cordeiro, P. (Eds.), 1as Jornadas Atlânticas de Protecção do Meio Ambiente. Angra do Heroísmo: Secretaria Regional do Turismo e Ambiente.
McClain, C.R., Lundsten, L., 2015. Assemblage structure is related to slope and depth on a deep offshore Pacific seamount chain. Mar. Ecol. 36, 210–220. https://doi.org/10.1111/maec.12136.
Medialdea, T., Somoza, L., Pinheiro, L.M., Fernández-Puga, M.C., Vázquez, J.T., León, R., Ivanov, M.K., Magalhaes, V., Díaz-del-Río, V., Vegas, R., 2009. Tectonics and mud volcano development in the Gulf of Cádiz. Mar. Geol. 261, 48–63. https://doi.org/10.1016/j.margeo.2008.10.007.
Metaxas, A., Lacharité, M., de Mendonça, S.N., 2019. Hydrodynamic connectivity of habitats of deep-water corals in Corsair Canyon, Northwest Atlantic: a case for cross-boundary conservation. Front. Mar. Sci. 6, 1–19. https://doi.org/10.3389/fmars.2019.00159.
Mienis, F., de Stigter, H.C., White, M., Dulneveldc, G., de Haas, H., van Weering, T.C.E., 2007. Hydrodynamic controls on cold-water coral growth and carbonate-mound development at the SW and SE rockall trough margin, NE Atlantic ocean. Deep. Res. Part I Oceanogr. Res. 54, 1655–1674. https://doi.org/10.1016/j.dsr.2007.05.013.
Miller, K.J., Gunasekera, R.M., 2017. A comparison of genetic connectivity in two deep sea corals to examine whether seamounts are isolated islands or stepping stones for dispersal. Sci. Rep. 7, 46103. https://doi.org/10.1038/srep46103.
Millot, C., 1999. Circulation in the western Mediterranean Sea. J. Mar. Syst. 20, 423–442. https://doi.org/10.1016/S0924-7963(98)00078-5.
Monniot, C., Monniot, F., 1988. Ascidies profondes de chaque côté du seuil de Gibraltar (Campagne BALGIM). Bull. Museum Natl. Hist. Nat. 3, 415–428.
Morato, T., Kvile, K., Taranto, G.H., Tempera, F., Narayanaswamy, B.E., Hebbeln, D., Menezes, G.M., Wienberg, C., Santos, R.S., Pitcher, T.J., 2013. Seamount physiography and biology in the North-East Atlantic and Mediterranean Sea. Biogeosciences 10, 3039–3054. https://doi.org/10.5194/bg-10-3039-2013.
Mosquera-Giménez, Á., Vélez-Belchí, P., Rivera, J., Piñeiro, S., Fajar, N., Caínzos, V., Balbín, R., Jiménez Aparicio, J.A., Dominguez-Carrió, C., Blasco-Ferre, J., Carreiro-Silva, M., Morato, T., Puerta, P., Orejas, C., 2019. Ocean circulation over North Atlantic underwater features in the path of the mediterranean outflow water : the Ormonde and Formigas seamounts , and the Gazul mud volcano. Front. Mar. Sci. 6, 1–18. https://doi.org/10.3389/fmars.2019.00702.
Moura, C.J., 2015. The hydrozoan fauna (Cnidaria: Hydrozoa) from the peaks of the Ormonde and Gettysburg seamounts (Gorringe bank, NE atlantic). Zootaxa 3972, 148–180. https://doi.org/10.11646/zootaxa.3972.2.2.
OCEANA, 2005. The seamounts of the Gorringe bank. Fond. Ermenegildo Zegna-Oceana 72. https://doi.org/10.1016/0038-092X(86)90130-1.
Oksanen, J., Blanchet, F.G., Friendly, M., Kindt, R., Legendre, P., McGlinn, D., Minchin, P.R., O'Hara, R.B., Simpson, G.L., Solymos, P., Stevens, M.H.H., Szoecs, E., Wagner, H., 2019. Vegan: community ecology package.
Orejas, C., Addamo, A., Alvarez, M., Aparicio, A., Alcoverro, D., Arnaud-Haond, S., Bilan, M., Boavida, J., Cainzos, V., Calderon, R., Cambeiro, P., Castano, M., Fox, A., Gallardo, M., Gori, A., Guitierrez, C., Henry, L.-A., Hermida, M., Jimenez, J.A., Lopez-Jurado, J.L., Lozano, P., Mateo-Ramirez, A., Mateu, G., Matoso, J.L., Mendez, C., Morillas, A., Movilla, J., Olariaga, A., Paredes, M., Pelayo, V., Pineiro, S., Rakka, M., Ramirez, T., Ramos, M., Reis, J., Rivera, J., Romero, A., Rueda, J.L., Salvador, T., Sampaio, I., Sanchez, H., Santiago, R., Serrano, A., Taranto, G., Urra, J., Velez-Belchi, P., Viladrich, N., Zein, M., 2017. Cruise report MEDWAVES survey (MEDiterranean out flow WAter and vulnerable EcosystemS)-. https://doi.org/10.5281/ZENODO.556516.
Paliy, O., Shankar, V., 2016. Application of multivariate statistical techniques in microbial ecology. Mol. Ecol. 25, 1032–1057. https://doi.org/10.1111/mec.13536.
Palomino, D., López-González, N., Vázquez, J.-T., Fernández-Salas, L.M., Rueda, J.L., Sánchez-Leal, R., Díaz-del-Río, V., 2016. Multidisciplinary study of mud volcanoes

and diapirs and their relationship to seepages and bottom currents in the Gulf of Cádiz continental slope (northeastern sector). Mar. Geol. 378, 196–212. https://doi.org/10.1016/j.margeo.2015.10.001.

Patarnello, T., Volckaert, F.A.M.J., Castilho, R., 2007. Pillars of hercules: is the atlantic-mediterranean transition a phylogeographical break? Mol. Ecol. 16, 4426–4444. https://doi.org/10.1111/j.1365-294X.2007.03477.x.

Pérès, J.M., 1985. History of the Mediterranean biota and the colonization of the depths. In: Margalef, R. (Ed.), Western Mediterranean. Pergamon Press, Oxford, pp. 198–232.

Pérès, J.M., Piccard, J., 1964. Nouveau manuel de bionomie benthique de la mer Mediterranée. Extr. du Recl. des Trav. la Stn. Mar. d'Endoume Bulletin 3, 1–137.

Pham, C.K., Canha, A., Diogo, H., Pereira, J.G., Prieto, R., Morato, T., 2013. Total marine fishery catch for the Azores (1950–2010). ICES J. Mar. Sci. 70, 564–577. https://doi.org/10.1093/icesjms/fst024.

Pollard, R.T., Read, J.F., Holliday, N.P., Leach, H., 2004. Water masses and circulation pathways through the Iceland Basin during Vivaldi 1996. J. Geophys. Res. Ocean. 109, C04004 https://doi.org/10.1029/2003JC002067.

Porteiro, F.M., Gomes-Pereira, J.N., Pham, C.K., Tempera, F., Santos, R.S., 2013. Distribution and habitat association of benthic fish on the Condor seamount (NE Atlantic, Azores) from in situ observations. Deep. Res. Part II Top. Stud. Oceanogr. 98, 114–128. https://doi.org/10.1016/j.dsr2.2013.09.015.

Puerta, P., Johnson, C., Carreiro-silva, M., Henry, L., Kenchington, E., Morato, T., Kazanidis, G., Rueda, J.L., Urra, J., Ross, S., Wei, C., González-irusta, J.M., Arnaud-Haond, S., Orejas, C., 2020. Influence of water masses on the biodiversity and biogeography of deep-sea benthic ecosystems in the north atlantic 7, 1–25. https://doi.org/10.3389/fmars.2020.00239.

Pusceddu, A., Bianchelli, S., Martín, J., Puig, P., Palanques, A., Masqué, P., Danovaro, R., 2014. Chronic and intensive bottom trawling impairs deep-sea biodiversity and ecosystem functioning. Proc. Natl. Acad. Sci. U. S. A, 201405454.

R Core Team, 2020. R: A Language and Environment for Statistical Computing.

Raddatz, J., Rüggeberg, A., 2019. Constraining past environmental changes of cold-water coral mounds with geochemical proxies in corals and foraminifera. Depositional Rec 200–222. https://doi.org/10.1002/dep2.98.

Raddatz, J., Rüggeberg, A., Liebetrau, V., Foubert, A., Hathorne, E.C., Fietzke, J., Eisenhauer, A., Dullo, W.-C., 2014. Environmental boundary conditions of cold-water coral mound growth over the last 3 million years in the Porcupine Seabight, Northeast Atlantic. Deep Sea Res. Part II Top. Stud. Oceanogr. 99, 227–236. https://doi.org/10.1016/j.dsr2.2013.06.009.

Radice, V.Z., Quattrini, A.M., Wareham, V.E., Edinger, E.N., Cordes, E.E., 2016. Vertical water mass structure in the North Atlantic influences the bathymetric distribution of species in the deep-sea coral genus Paramuricea. Deep. Res. Part I Oceanogr. Res. 116, 253–263. https://doi.org/10.1016/j.dsr.2016.08.014.

Ramalho, R.S., Quartau, R., Madeira, J., Rebelo, A.C., 2018. The geology of Formigas islets and its significance to our comprehension of the Terceira rift in the azores triple junction. AGU Fall Meeting Abstracts 2018, V23L, 0207.

Ramos, M., Calado, G., Bertocci, I., Tempera, F., Duarte, P., Albuquerque, M., 2016. Patterns in megabenthic assemblages on a seamount summit (Ormonde peak, Gorringe bank, northeast atlantic). Mar. Ecol. 37, 1057–1072. https://doi.org/10.1111/maec.12353.

Reveillaud, J., Freiwald, A., Van Rooij, D., Le Guilloux, E., Altuna, A., Foubert, A., Vanreusel, A., Roy, K.O.-L., Henriet, J.-P., 2008. The distribution of scleractinian corals in the Bay of Biscay, NE Atlantic. Facies 54, 317–331. https://doi.org/10.1007/s10347-008-0138-4.

Roberts, E., Bowers, D., Meyer, H., Samuelsen, A., Rapp, H., Cárdenas, P., 2021. Water masses constrain the distribution of Deep-sea sponges in the north Atlantic Ocean and nordic seas. Mar. Ecol. Prog. Ser. 659, 75–96. https://doi.org/10.3354/meps13570.

Rogers, A.D., 2018. The biology of seamounts: 25 Years on. Adv. Mar. Biol. 79, 137–224. https://doi.org/10.1016/bs.amb.2018.06.001.

Rowden, A.A., Dower, J.F., Schlacher, T.A., Consalvey, M., Clark, M.R., 2010. Paradigms in seamount ecology: fact, fiction and future. Mar. Ecol. 31, 226–241.

Rueda, J.L., González-García, E., Marina, P., Oporto, T., Rittierott, C., López-González, N., Farias, C., Moreira, J., López, E., Megina, C., López-González, P.J., García Raso, J. E., Gofas, S., Salas, C., Bruque, G., López, F.J., Vázquez, J.T., Fernández-Salas, L.M., Díaz-del-Río, V., 2012. Biodiversity and geodiversity in the mud volcano field of the Spanish margin (Gulf of Cádiz) 137–141. https://doi.org/10.13140/2.1.3244.3849.

Sampaio, Í., Freiwald, A., Porteiro, F.M., Menezes, G., Carreiro-Silva, M., 2019. Census of octocorallia (cnidaria: anthozoa) of the azores (NE atlantic) with a nomenclature update. Zootaxa 4550, 451–498. https://doi.org/10.11646/zootaxa.4550.4.1.

Sánchez-Leal, R.F., Bellanco, M.J., Fernández-Salas, L.M., García-Lafuente, J., Gasser-Rubinat, M., González-Pola, C., Hernández-Molina, F.J., Pelegrí, J.L., Peliz, A., Relvas, P., Roque, D., Ruiz-Villarreal, M., Sammartino, S., Sánchez-Garrido, J.C., 2017. The mediterranean overflow in the Gulf of cadiz: a rugged journey. Sci. Adv. 3, 1–12. https://doi.org/10.1126/sciadv.aao0609.

Sánchez, F., González-Pola, C., Druet, M., García-Alegre, A., Acosta, J., Cristobo, J., Parra, S., Ríos, P., Altuna, Á., Gómez-Ballesteros, M., Muñoz-Recio, A., Rivera, J., del Río, G.D., 2014. Habitat characterization of deep-water coral reefs in La gaviera canyon (avilés canyon system, cantabrian sea). Deep. Res. Part II Top. Stud. Oceanogr. https://doi.org/10.1016/j.dsr2.2013.12.014.

Santos, R.S., Hawkins, S., Monteiro, L.R., Alves, M., Isidro, E.J., 1995. Marine research, resources and conservation in the Azores. Aquat. Conserv. Mar. Freshw. Ecosyst. 5, 311–354. https://doi.org/10.1002/aqc.3270050406.

Sitjá, C., Maldonado, M., Farias, C., Rueda, J.L., 2018. Deep-water sponge fauna from the mud volcanoes of the Gulf of cadiz (North Atlantic , Spain). J. Mar. Biol. Assoc. U. K. 1–25. https://doi.org/10.1017/S0025315418000589 Received.

Sitjà, C., Maldonado, M., Farias, C., Rueda, J.L., 2020. Export of bathyal benthos to the Atlantic through the Mediterranean outflow: sponges from the mud volcanoes of the Gulf of Cadiz as a case study. Deep. Res. Part I Oceanogr. Res. Pap. 163 https://doi.org/10.1016/j.dsr.2020.103326.

Sitjà, C., Maldonado, M., Farias, C., Rueda, J.L., 2019. Deep-water sponge fauna from the mud volcanoes of the Gulf of cadiz (North Atlantic, Spain). J. Mar. Biol. Assoc. U. K. 99, 807–831. https://doi.org/10.1017/S0025315418000589.

Somoza, L., Ercilla, G., Urgorri, V., León, R., Medialdea, T., Paredes, M., Gonzalez, F.J., Nombela, M.A., 2014. Detection and mapping of cold-water coral mounds and living Lophelia reefs in the Galicia Bank, Atlantic NW Iberia margin. Mar. Geol. 349, 73–90. https://doi.org/10.1016/j.margeo.2013.12.017.

Somoza, L., Rueda, J.L., Sánchez-Guillamón, O., Medialdea, T., Rincón-Tomás, B., González, F.J., Palomino, D., Madureira, P., López-Pamo, E., Fernández-Salas, L.M., Santofimia, E., León, R., Marino, E., Fernández-Puga, M., del, C., Vázquez, J.T., 2021. The interactive role of hydrocarbon seeps, hydrothermal vents and intermediate antarctic/mediterranean water masses on the distribution of some vulnerable deep-sea habitats in Mid latitude NE Atlantic Ocean. Oceans 2, 351–385. https://doi.org/10.3390/oceans2020021.

Templado, J., Calvo, M., Moreno, D., Flores, A., Conde, F., Abad, R., Rubio, J., López-Fé, C., Ortiz, M., 2006. Flora y fauna de la reserva marina y reserva de pesca de la isla de Alborán. Ministerio de Agricultura, Pesca y Alimentación. Secretaría General de Pesca, Madrid.

Templado, J., García-Carrascosa, M., Baratech, L., Capaccioni, R., Juan, A., López-Ibor, A., Silvestre, R., Massó, C., 1986. Estudio preliminar de la fauna asociada a los fondos coralígenos del mar de Alborán (SE de España). Bol. Inst. Esp. Ocean. 3, 93–104.

UNGA, 2006. Resolution 61/105. Sustainable Fisheries, Including Through the 1995 Agreement for the Implementation of the Provisions of the United Nations Convention on the Law of the Sea of 10 December 1982 Relating to the Conservation and Management of Straddling Fish Stocks and Highly Migratory Fish Stocks, and Related Instruments. United Nations General Assembly. Available at: http://www.un.org/Depts/los/ general_assembly/general_assembly_reports.htm.

Urra, J., Palomino, D., Lozano, P., González-García, E., Farias, C., Mateo-Ramírez, Á., Fernández-Salas, L.M., López-González, N., Vila, Y., Orejas, C., Puerta, P., Rivera, J., Henry, L.-A., Rueda, J.L., 2021. Deep-sea habitat characterization using acoustic data and underwater imagery in Gazul mud volcano (Gulf of Cádiz, NE Atlantic). Deep-Sea Res. Part I Oceanogr. Res. Pap. 169, 103458 https://doi.org/10.1016/j.dsr.2020.103458.

van den Beld, I.M.J., Bourillet, J.-F., Arnaud-Haond, S., de Chambure, L., Davies, J.S., Guillaumont, B., Olu, K., Menot, L., 2017. Cold-water coral habitats in submarine canyons of the bay of biscay. Front. Mar. Sci. 4 https://doi.org/10.3389/fmars.2017.00118.

Van Rooij, D., Iglesias, J., Hernandez-Molina, F.J., Ercilla, G., Gomez-Ballesteros, M., Casas, D., Llave, E., De Hauwere, A., Garcia-Gil, S., Acosta, J., Henriet, J.P., 2010. The le danois contourite depositional system: interactions between the mediterranean outflow water and the upper cantabrian slope (north iberian margin). Mar. Geol. 274, 1–20. https://doi.org/10.1016/j.margeo.2010.03.001.

Victorero, L., Robert, K., Robinson, L.F., Taylor, M.L., Huvenne, V.A.I., 2018. Species replacement dominates megabenthos beta diversity in a remote seamount setting. Sci. Rep. 8, 1–11. https://doi.org/10.1038/s41598-018-22296-8.

Vieira, R.P., Raposo, I.P., Sobral, P., Gonçalves, J.M.S., Bell, K.L.C.C., Cunha, M.R., 2015. Lost fishing gear and litter at Gorringe bank (NE atlantic). J. Sea Res. 100, 91–98. https://doi.org/10.1016/j.seares.2014.10.005.

White, M., Dorschel, B., 2010. The importance of the permanent thermocline to the cold water coral carbonate mound distribution in the NE Atlantic. Earth Planet Sci. Lett. 296, 395–402. https://doi.org/10.1016/j.epsl.2010.05.025.

White, M., Dorschel, B., 2010. The importance of the permanent thermocline to the cold-water coral carbonate mound distribution in the NE Atlantic. Earth Planet Sci. Lett. 296, 395–402.

Wienberg, C., Wintersteller, P., Beuck, L., Hebbeln, D., 2013. Coral Patch seamount (NE Atlantic) - a sedimentological and megafaunal reconnaissance based on video and hydroacoustic surveys. Biogeosciences 10, 3421–3443. https://doi.org/10.5194/bg-10-3421-2013.

Xavier, J., Van Soest, R., 2007. Demosponge fauna of Ormonde and Gettysburg seamounts (Gorringe bank, north-east atlantic): diversity and zoogeographical affinities. J. Mar. Biol. Assoc. U. K. 87, 1643–1653. https://doi.org/10.1017/S0025315407058584.